© 2005 The Chemical Society of Japan

Award Accounts

The Chemical Society of Japan Award for Young Chemists for 2003

Development of an Antiferromagnetic Organic Superconductor κ-(BETS)$_2$FeBr$_4$

Hideki Fujiwara* and Hayao Kobayashi[1]

Research Institute for Advanced Science and Technology, Osaka Prefecture University, Gakuen-cho 1-2, Sakai 599-8570

[1]Institute for Molecular Science, Myodaiji, Okazaki 444-8585

Received November 10, 2004; E-mail: hfuji@c.s.osakafu-u.ac.jp

The first antiferromagnetic organic superconductor, κ-(BETS)$_2$FeBr$_4$ [BETS = bis(ethylenedithio)tetraselenafulvalene], was developed in the search for novel magnetic molecular conductors. This salt shows successive antiferromagnetic and superconducting transitions at $T_N = 2.5$ K and $T_c = 1.1$ K, respectively, at ambient pressure. Specific heat measurements and anisotropic behavior of intraplanar conducting properties under applied magnetic fields prove the coexistence of the antiferromagnetic ordering and superconductivity below T_c. The combination of metamagnetism of the magnetic layer and superconductivity of the conduction layer, which makes this salt a dual-functional system, yields two characteristic magnetic field-induced superconducting states around 1.6 and 12.5 T in terms of the Jaccarino–Peter compensation effect. Systematic studies on both the chemical pressure effect by a halogen exchange in the alloy system κ-(BETS)$_2$FeBr$_x$Cl$_{4-x}$ and the physical pressure effect by an application of real pressures in κ-(BETS)$_2$FeBr$_4$ were performed to discuss the π–d interaction in the κ-(BETS)$_2$FeBr$_4$ system.

Since the discovery in 1973 of the first organic metallic charge-transfer complex, TTF–TCNQ (tetrathiafulvalene–tetracyano-*p*-quinodimethane),[1] the development of organic conducting materials based on TTF-type donor molecules has made great advances in the fields of chemistry and physics.[2–5] In particular, the discoveries of superconductivities in the cation radical salts based on tetramethyltetraselenafulvalene (TMTSF) in 1980 and in those based on bis(ethylenedithio)-TTF (BEDT-TTF) in 1983 have directed considerable attention to the development of new π-electron donors.[6,7] The designability of organic systems has encouraged many chemists to produce numerous types of novel conducting systems.[2,4] Although organic conducting materials have complicated molecular and crystal structures, the resultant electronic structures are quite simple, so organic conductors are regarded by physicists as a adequate system for the investigation of electronic states and well-defined Fermi surfaces by physical measurements, including Shubnikov–de Haas (SdH) and de Haas–van Alphen (dHvA) oscillations.[8] Among the materials, BEDT-TTF, synthesized for the first time in 1978,[9] has played the most important role in the development of organic conductors and has yielded many organic superconductors such as κ-type BEDT-TTF superconductors so far. In these, transverse intermolecular S–S networks play an essential role to form a two-dimensional electronic structure and to stabilize the resultant metallic states.[3,10] Crystal structures of several kinds of BEDT-TTF salts have been classified by T. Mori.[11] Among the κ-type BEDT-TTF salts, κ-(BEDT-TTF)$_2$I$_3$ was reported by A. Kobayashi et al. (superconducting critical temperature, $T_c = 3.6$ K) in 1987 as the first superconductor exhibiting a characteristic two-dimensional κ-type arrangement,[12] and Urayama and co-workers reported the first organic superconductor that has a T_c higher than 10 K, κ-(BEDT-TTF)$_2$Cu(NCS)$_2$ ($T_c = 10.4$ K at ambient pressure) in 1988.[13] Very recently, Taniguchi et al. discovered the highest T_c in the organic superconductors under high pressure of 8.2 GPa in β'-(BEDT-TTF)$_2$ICl$_2$ at 14.2 K (Chart 1).[14]

Molecular materials are considered to be a suitable system for constructing novel functional materials by combining several kinds of molecular building blocks that have different functionalities like electrical conductivity, magnetism or optical properties. Several approaches using TTF frameworks as building blocks have been extensively studied to explore systems capable of acting as sensors, liquid crystals, catalysts, or

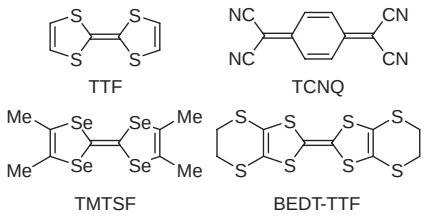

Chart 1.

Published on the web July 1, 2005; DOI 10.1246/bcsj.78.1181

switching devices in the fields of macrocyclic and supramolecular chemistry.[15] A considerable amount of interest is also focused on the hybrid systems that consist of π donor molecules and inorganic magnetic anions to investigate the "dual-functional system" between the conductivity and magnetism that comes from the interplay of π and d electron systems, namely, a "π–d interaction".[16] Such a system was firstly reported in (BEDT-TTF)$_3$CuCl$_4$·H$_2$O in the early 1990's, in which BEDT-TTF molecules construct a stable metallic state down to 0.2 K and Cu^{2+} localized spins show a weak short-range ferromagnetic interaction.[17] In 1995, β''-(BEDT-TTF)$_4$(H$_3$O)[Fe(C$_2$O$_4$)$_3$](C$_6$H$_5$CN) was proved to be the first paramagnetic organic superconductor by Day and co-workers,[18] and the first organic ferromagnetic metal, (BEDT-TTF)$_3$[MnCr(C$_2$O$_4$)$_3$] was discovered by Coronado's group in 2000.[19] However, in these systems, there is almost no correlation between the conductivity and magnetism and these two functionalities work independently in the crystals. Usually the magnetic interaction through the π–d interaction between the π-conduction electrons that originate from the TTF-like π donors and the d-localized spins located on the magnetic transition metal anion is very small (usually smaller than 10 K order). Therefore, the stabilization of metallic states down to low temperature is of considerable importance to investigate the dual-functionality between the metallic conductivity/superconductivity and magnetism. We focused on a selenium-containing donor, BETS [= bis(ethylenedithio)tetraselenafulvalene], in which four sulfur atoms of the TTF core of BEDT-TTF are substituted by four selenium atoms, because BETS has a strong tendency to form a stable metallic state down to liquid helium temperatures.[20] Then, we started the development of organic metals with magnetic anions like $FeCl_4^-$ and $FeBr_4^-$ to study the interplay of the π-conduction electrons and the d-localized magnetic moments.[21] BETS conductors containing magnetic Fe^{3+} ions were found to show a variety of electromagnetic properties.[22] Firstly, we investigated needle-shaped crystals of BETS salts involving transition metal halides: λ-(BETS)$_2$MCl$_4$ (M = Ga and Fe). Though non-magnetic $GaCl_4^-$ salt exhibits a rather simple superconducting transition at T_c of 6 K,[23] λ-(BETS)$_2$FeCl$_4$ is a remarkable conductor showing surprisingly rich electronic properties. It undergoes a π–d coupled antiferromagnetic insulating transition at 8.5 K at ambient pressure.[24] However, it recovers its metallic behavior under magnetic fields above 11 T, where Fe^{3+} spins are in a forced-ferromagnetic orientation, and then takes a novel field-induced superconducting state over the broad field range of 18–42 T for the applied magnetic fields exactly parallel to the conduction plane.[25] In addition, it becomes a superconductor at high pressure by suppressing the antiferromagnetic insulating state.[26] Furthermore, in the alloy system, λ-(BETS)$_2$Fe$_x$Ga$_{1-x}$Cl$_4$ where magnetic Fe^{3+} moments are diluted with non-magnetic Ga^{3+} ions, an unprecedented superconductor-to-insulator transition was observed around $x \approx 0.5$ as a result of the competition between the superconducting state and the antiferromagnetic insulating state.[27]

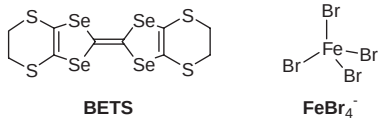

Chart 2.

There is another important modification of BETS salts with the κ-type structure: κ-(BETS)$_2$MX$_4$ (M = Fe and Ga, X = Cl and Br). Since the discovery of the first κ-type organic superconductor among the BEDT-TTF salts, the κ-type structure has been recognized to be a very suitable structure to stabilize metallic states. Several κ-type BETS salts have been studied so far.[20,21,28] Among many κ-type BETS salts that we investigated, κ-(BETS)$_2$GaBr$_4$ shows a superconducting transition at T_c of 0.5–1.0 K.[29] On the other hand, κ-(BETS)$_2$FeBr$_4$ that has magnetic Fe^{3+} spins was revealed to be the first antiferromagnetic organic superconductor; the successive antiferromagnetic and superconducting transitions are observed at 2.5 K and 1.1 K, respectively. Here, recent results on the structures, magnetic and electrical properties of the first antiferromagnetic organic superconductor: κ-(BETS)$_2$FeBr$_4$ are presented (Chart 2).[30] We also investigated the magnetic field dependence of the electrical resistivities and pursued the possibility for switching of conducting properties by external magnetic fields and field-induced superconductivities.[31] Furthermore, the physical properties of the alloy system κ-(BETS)$_2$FeBr$_x$Cl$_{4-x}$ ($0 \leq x \leq 4$) and the pressure dependence of the conducting behavior of κ-(BETS)$_2$FeBr$_4$ are also investigated to discuss the π–d interaction in κ-(BETS)$_2$FeBr$_4$.[32,33]

1. Crystal Structure, Band Structure, and Fermi Surface of κ-(BETS)$_2$FeBr$_4$

Synthesis of BETS was performed according to the method previously reported by Kato et al.[20] However, an available short-cut method for the synthesis of the intermediate, 2,3-dihydro-1,4-dithiin, was reported by Malfant et al.[34] Preparation of single crystals of the $FeBr_4$ salts of BETS was carried out electrochemically under a constant current of 0.7 μA at 40 °C in a chlorobenzene–ethanol solution (9:1 vol/vol) containing BETS and tetraethylammonium iron(III) tetrabromide that was prepared by mixing iron(III) tribromide and tetraethylammonium bromide in hot ethanol.[30b] Black plates and black needles were grown from the anode electrode after several weeks and were determined to be κ-(BETS)$_2$FeBr$_4$ and λ'-(BETS)$_2$FeBr$_4$ salts by X-ray crystallographic analyses, respectively.[35]

Figure 1 shows the crystal structure of κ-(BETS)$_2$FeBr$_4$.[30b] The κ-(BETS)$_2$FeBr$_4$ salt belongs to orthorhombic, *Pnma* space group with crystal lattice parameters: $a = 11.787(6)$, $b = 36.607(9)$, $c = 8.504(5)$ Å, $V = 3669(2)$ Å^3, $Z = 8$ at room temperature. As Fig. 1b indicates, the BETS molecules form dimers, overlapping each other in a "ring-over-bond" manner, and adjacent BETS dimers are arranged in a roughly orthogonal manner that is characteristic of the "κ-type packing motif".[3,11b] There is no essential difference of molecular arrangements between κ-(BETS)$_2$FeBr$_4$ and κ-(BETS)$_2$FeCl$_4$.[21] There is only one Se···Se contact shorter than the sum of the van der Waals (vdW) radii of selenium atom, 3.796(3) Å, and several short Se···S and S···S contacts (the shortest ones are 3.593(6) and 3.362(8) Å, respectively) between the donor dimers, as shown in Fig. 1b, suggesting that a two-dimensional intermolecular network is developed in the donor layer. The

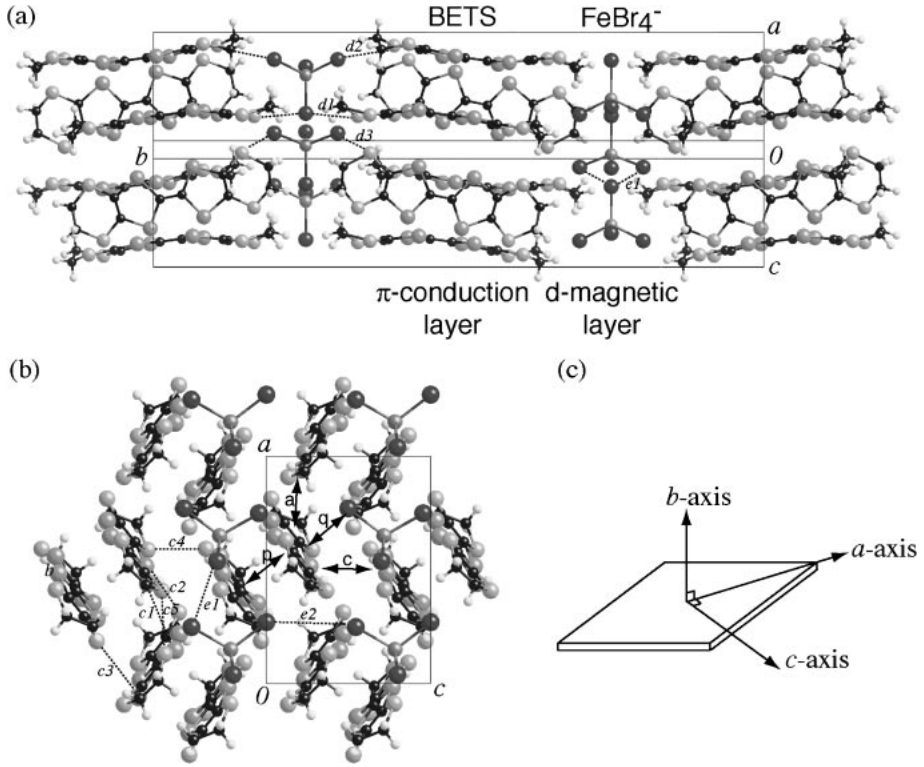

Fig. 1. (a) Crystal structure of κ-$(BETS)_2FeBr_4$ where π-conduction layers of the BETS molecules and d-magnetic layers of the $FeBr_4^-$ anions are arranged alternately along the *b*-direction. (b) Crystal structure projected along the *b*-axis. Short chalcogen–chalcogen contacts: *c1* [Se(1)–Se(2)] = 3.796(3), *c2* [Se(3)–S(4)] = 3.593(6), *c3* [Se(1)–S(4)] = 3.656(5), *c4* [S(1)–S(3)] = 3.362(8), and *c5* [S(1)–S(2)] = 3.369(8) Å. Short distances: *d1* [Br(3)–S(2)] = 3.693(6), *d2* [Br(1)–S(3)] = 3.708(6), *d3* [Br(1)–S(1)] = 3.776(6), *e1* [Br(1)–Br(3)] = 4.137(4), and *e2* [Br(2)–Br(3)] = 4.637(5) Å. Overlap integrals; p 77.33, a −22.41, c 35.14, and q 8.11 × 10^{-3}. (c) Schematic drawing of the crystal habit indicating the crystallographic three principal axes.

BETS dimers form two-dimensional conduction layers in the *ac*-plane, and the insulating layers of the $FeBr_4^-$ anions are sandwiched by the donor layers along the *b*-direction (Fig. 1a). In the anion layer, the nearest Fe···Fe distances are quite long values of 5.921(3) Å along the *a*-axis and 8.504(5) Å along the *c*-axis, suggesting that the direct dipole–dipole interaction between the Fe^{3+} moments can be almost neglected. On the other hand, the shortest Br···Br distance along the *a*-axis is 4.137(4) and is much shorter than that along the *c*-axis, 4.637(5) Å, but these distances are still longer than the sum of the vdW radii of bromines (3.7 Å). These results suggest that the intermolecular interaction between the anion molecules is weak, but is relatively stronger along the *a*-axis compared to that along the *c*-axis. In the case of the λ-$(BETS)_2FeCl_4$ salt, which shows a very strong π–d interaction that results in the π–d coupled antiferromagnetic insulating transition, there is a short contact between the selenium atom of the TSF core and the chlorine atom of the anion (Cl···Se; 3.528 Å).[21] However, no Br···Se short contact is observed in the κ-$(BETS)_2FeBr_4$ salt and there are several short Br···S contacts between BETS and the anion molecules, as indicated in Fig. 1a (the shortest Br–S distance is 3.693(6) Å). Therefore, the interaction between the π-conduction electrons of the BETS layer and the d-localized spins of the magnetic anion layer in the κ-$(BETS)_2FeBr_4$ salt is weaker than in the case of the λ-$(BETS)_2FeCl_4$ salt.

A tight-binding band structure was calculated based on the extended Hückel approximation using the room temperature structural data.[30b,36] The obtained band dispersion and Fermi surface are shown in Fig. 2. Reflecting the dimer structure of the κ-type salts, the intradimer overlap integral (p; 77.33 × 10^{-3}) of the κ-$(BETS)_2FeBr_4$ salt is much larger than the other overlaps (a; −22.41, q; 8.11, and c; 35.14 × 10^{-3}). The band dispersion of κ-$(BETS)_2FeBr_4$ has four energy branches, and there is a mid-gap between the upper two branches and the lower two branches due to the strong dimerization of the donor molecules. Consequently the upper band becomes effectively a half-filled one, suggesting a strongly correlated electronic structure of this salt. The calculated Fermi surface is a two-dimensional circle and is closed in the XV boundary, similar to the surfaces of the isostructural κ-$(BETS)_2FeCl_4$ and κ-$(BETS)_2GaCl_4$ salts, whose SdH oscillations were already investigated and shown to be consistent with the calculated

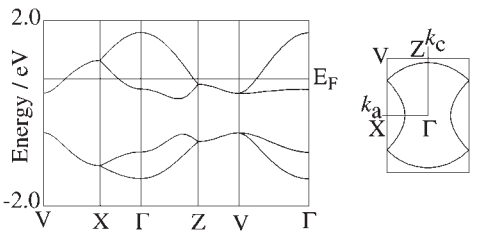

Fig. 2. Band structure and Fermi surface of κ-$(BETS)_2FeBr_4$.

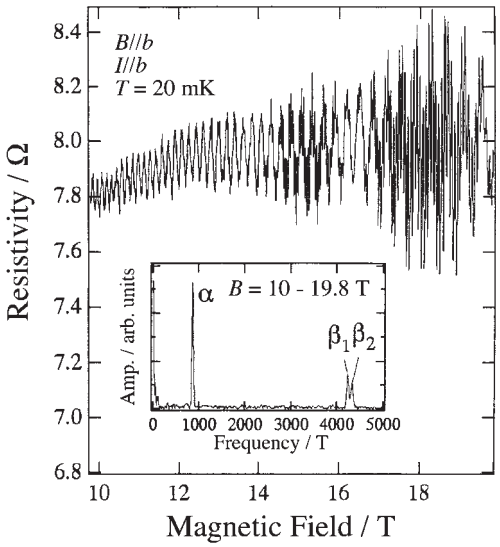

Fig. 3. Field dependence of magnetoresistances of κ-$(BETS)_2FeBr_4$ in the field range of 10–19.8 T at 20 mK applied perpendicular to the conduction plane ($\parallel$ *b*-axis). The inset shows the Fourier transform spectrum in this field range (From Ref. 39b).

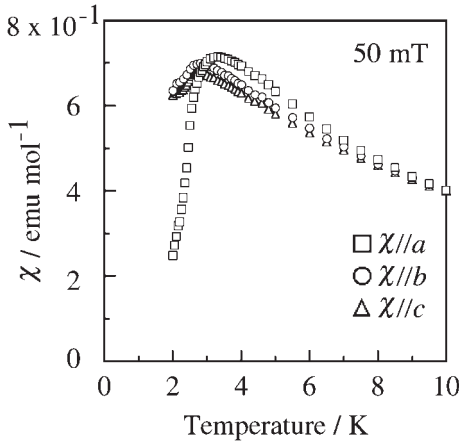

Fig. 4. Temperature dependence of magnetic susceptibilities (χ) of a plate-like single crystal of κ-$(BETS)_2FeBr_4$ at 50 mT. $\chi \parallel a$ (opened squares), $\chi \parallel b$ (opened circles), and $\chi \parallel c$ (opened triangles) represent the magnetic susceptibilities under the fields applied to the crystallographic *a*-, *b*-, and *c*-axes, respectively.

Fermi surfaces.[37] The effect of the localized Fe^{3+} spins on the two-dimensional electronic system of λ- and κ-type BETS salts has been theoretically examined by Hotta et al. based on the calculation with the mean-field approximation for the on-site Coulombic interaction, suggesting that κ-$(BETS)_2FeBr_4$ has a spin density wave (SDW)-like ground state.[38]

In the case of κ-$(BETS)_2FeBr_4$, SdH oscillation measurements were performed by Uji et al.[39] When the magnetic field was applied perpendicular to the conduction plane ($\parallel$ *b*-axis), the resistivity measured perpendicular to the conduction plane shows clear SdH oscillations, as shown in Fig. 3. After the Fourier transformation, three different oscillations (α, β_1, and β_2) are observed at 850, 4230, and 4330 T, respectively, as shown in the inset of Fig. 3. The cross-sectional areas corresponding to the α and β (β_1 or β_2) are estimated to be about 20% and 100% of the first Brillouin zone, respectively. Contrary to the band calculation based on the room temperature structural data, the observation of the α orbit indicates that the gap opens in the XV zone boundary; the β oscillation corresponds to a magnetic break-down orbit, suggesting the presence of some structural phase transition at low temperature. The origin of the splitting phenomena of the β orbit (β_1 and β_2) will be discussed later (section 6).

2. Magnetic Properties of κ-$(BETS)_2FeBr_4$

We examined the magnetic properties of the κ-$(BETS)_2FeBr_4$ salt using a SQUID magnetometer.[30b] Static magnetic susceptibilities were measured on a plate-shaped single crystal of κ-$(BETS)_2FeBr_4$ to estimate the anisotropy of the magnetic properties by applying a magnetic field (50 mT) along the three crystallographic axes of the single crystal (the *a*-, *b*-, and *c*-axes). The obtained magnetic susceptibilities at 100–300 K can be well fitted by the Curie–Weiss plot and give a negative Weiss temperature ($\theta = -5.5$ K), suggesting that the dominant magnetic interaction is an antiferromagnetic one. The obtained Curie constant ($C = 4.70$ emu K mol^{-1}) exhibits that the iron(III) atom of the $FeBr_4^-$ anion is in a high-spin state. Figure 4 shows the temperature dependence of susceptibilities (χ) in the temperature range of 2 to 10 K.

All the magnetic susceptibilities along the three axes ($\chi \parallel a$, $\chi \parallel b$, and $\chi \parallel c$) take a similar maximum around 3 K. However, only $\chi \parallel a$ exhibits a fairly sharp decrease of susceptibilities below 2.5 K, while $\chi \parallel b$ and $\chi \parallel c$ tend to be constant as the temperature decreases. These results indicate that an antiferromagnetic ordering of Fe^{3+} spins occurs around 2.5 K ($\approx T_N$; Néel temperature) with an easy spin axis parallel to the *a*-axis. That is, κ-$(BETS)_2FeBr_4$ is the first organic conductor with an antiferromagnetic metal phase at ambient pressure, because this salt retains its metallic state below 2.5 K, as described later (section 3). On the other hand, the magnetic field dependence of magnetizations (*M*) was measured at 2.0 K, as shown in Fig. 5. The magnetization with the field applied parallel to the *a*-axis ($M \parallel a$) begins to show a rapid increase from 1.0 T at 2.0 K, then, saturates to the calculated value of the $S = 5/2$ spin system at 3.0 T. On the other hand, when the magnetic field is applied in parallel to the *b*- and *c*-axes, the magnetizations ($M \parallel b$ and $M \parallel c$) increase linearly as the field increases and tend to saturate around 6.0 T. These results suggest that a metamagnetic transition takes place around 1.5 T only when the field is applied parallel to the easy axis of the antiferromagnetic ordering (the *a*-axis). As mentioned in the crystal structure of the κ-$(BETS)_2FeBr_4$ salt, the direct intermolecular interaction between the anions along the *a*-axis seems to be strong and dominant compared to the cases along the other axes. However, the interlayer magnetic interaction through the π–d interaction, though considered to be relatively small, should be taken into account to explain the appearance of the bulk antiferromagnetic transition.

3. Conducting Properties of κ-$(BETS)_2FeBr_4$

In the previously reported paper,[21] the conducting properties of the κ-$(BETS)_2FeBr_4$ salt were examined down to 4.2 K. A

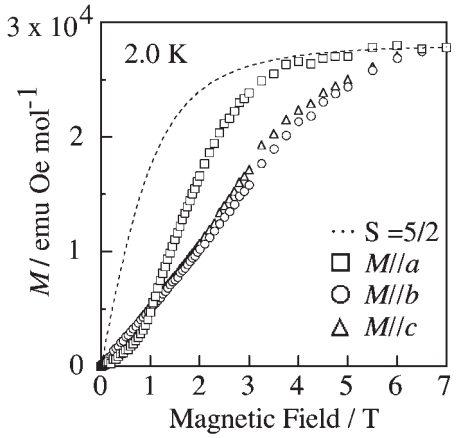

Fig. 5. Magnetic field dependence of magnetizations (M) at 2.0 K of a plate-like single crystal of κ-$(BETS)_2FeBr_4$. $M \parallel a$ (opened squares), $M \parallel b$ (opened circles), and $M \parallel c$ (opened triangles) represent the magnetizations for the fields applied along the three axes of crystal lattice. A Brillouin function calculated for $g = 2$ and $S = 5/2$ system is also shown as a dotted line for comparison.

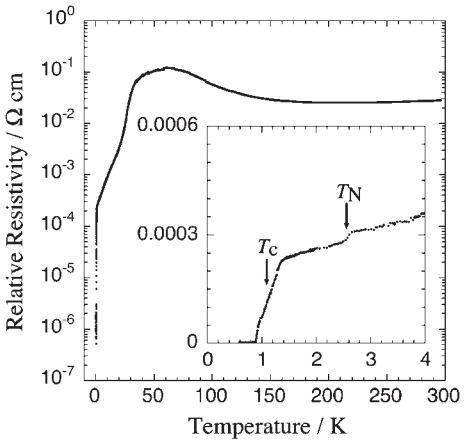

Fig. 6. Temperature dependence of relative resistivities of κ-$(BETS)_2FeBr_4$ at 0.6–300 K measured along the *ac*-plane at zero field. (Inset: in the temperature range between 0.6 and 4 K.)

large decrease of resistivities even around liquid helium temperature was found as the temperature decreased. Therefore, to examine the detailed conducting properties, especially at low temperatures, we measured the electrical resistivities of κ-$(BETS)_2FeBr_4$ down to 0.6 K using a ^{3}He cryostat and a superconducting magnet.[30b] Figure 6 shows the temperature dependence of relative resistivities at ambient pressure. This salt shows a very high electrical conductivity of 36 $S\,cm^{-1}$ at room temperature. The resistivity decreases very slowly from room temperature to about 200 K. Contrary to the normal metallic behavior of κ-$(BETS)_2FeCl_4$,[21] κ-$(BETS)_2FeBr_4$ with a large size of iron tetrabromide anion shows a gradual increase of resistivities below 200 K and takes a characteristic peak around 60 K, below which the resistivity decreases very rapidly by several orders. Such a resistivity peak has often been observed in the κ-type BEDT-TTF superconducting salts and is a characteristic behavior of the strong electron correlation systems that have a strongly dimerized κ-type donor arrangement. Indeed, the calculation of the intermolecular overlap integrals based on the extended Hückel approximation revealed that the intradimer interaction of the κ-$(BETS)_2FeBr_4$ salt (p; 77.33×10^{-3}) is stronger than that of the κ-$(BETS)_2FeCl_4$ salt (64.37×10^{-3}), which shows no resistivity peak around 60 K.[21]

As seen from the inset of Fig. 6, the resistivity shows a small step-like decrease around 2.5 K where the antiferromagnetic transition of the Fe^{3+} spins takes place. This clearly shows that the resistivity is depressed by the disappearance of magnetic scattering due to the antiferromagnetic ordering of the Fe^{3+} spins and can be regarded as direct evidence for the important role of the interaction between π-conduction electrons and d-localized magnetic moments. Furthermore, a superconducting transition was observed at 1.1 K. In the cases of the λ-type alloy system, λ-$(BETS)_2Fe_xGa_{1-x}Br_yCl_{4-y}$ ($0.35 < x < 1$, $y < 0.5$), which also shows both superconducting and antiferromagnetic transitions, the superconducting state is broken by the development of antiferromagnetic ordering of Fe^{3+} spins to result in the superconductor-to-insulator or superconductor-to-metal transitions, and superconductivity and antiferromagnetism can not coexist.[27] However, κ-$(BETS)_2FeBr_4$ undergoes the transition from the antiferromagnetic metal phase to the superconducting phase.

To examine the conducting properties under magnetic fields, we measured the electrical resistivities along the *a*-axis of a plate-like single crystal under the magnetic field applied along the crystallographic three axes: $H \parallel a$, $H \parallel b$, and $H \parallel c$ below 5 K. The temperature dependences of resistivities under magnetic fields are plotted in Figs. 7a, b, and c. When we applied the magnetic fields along the easy axis of the antiferromagnetic transition ($H \parallel a$), the resistivity drop at T_N ($\approx$2.5 K) under zero magnetic field shifts quickly to the lower temperatures and disappears at 1.8 T. On the other hand, when we applied the magnetic fields along the *b*- and *c*-axes (the magnetic hard-axes), the temperature shifts of the resistivity drop are very small up to 1.0 T and then the drop gradually moves to the lower temperatures and vanishes at 4.0 T. The magnetic field dependence of the temperature of the resistivity drops is completely the same as that of the Néel temperatures (T_N) measured by a SQUID magnetometer. These results prove that the resistivity drops at the Néel temperature originate from the antiferromagnetic ordering of the Fe^{3+} localized spins and that there is π–d interaction between the BETS π-conduction electron system and the Fe^{3+} d-spin system. Furthermore, the temperature dependence of the resistivities is still metallic under magnetic fields over 3.0 T along the *a*-axis. It is thus clear that the metallic state coexists with the forced ferromagnetic state metamagnetically induced by the applied magnetic field.

A sharp superconducting transition is observed at 1.1 K under zero magnetic field and is suppressed by the application of a magnetic field. However, the suppression of the superconducting transition exhibits a remarkable anisotropy in terms of the direction of the applied magnetic fields. As shown in Fig. 7b, when the magnetic field is applied perpendicular to the conduction *ac*-plane ($H \parallel b$), the superconducting state is quickly broken and normal metallic state is recovered at weak

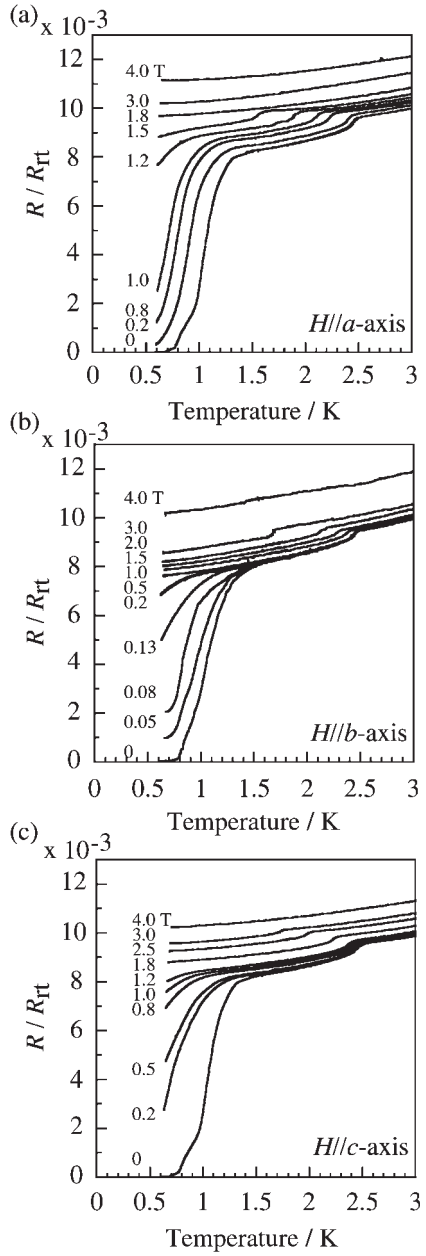

Fig. 7. Temperature dependence of normalized electrical resistivities (R/R_{rt}) of κ-$(BETS)_2FeBr_4$ at 0.6–3.0 K measured along the *a*-axis under the indicated magnetic fields applied (a) along the *a*-axis, (b) along the *b*-axis, and (c) along the *c*-axis.

magnetic fields over 0.2 T. This is consistent with the cases of the κ-type two-dimensional organic superconductors like the κ-$(BEDT\text{-}TTF)_2X$ salts,[3] in which the superconducting state is quite anisotropic and the upper critical field when the field is applied perpendicular to the conduction plane is considerably smaller than that for the case applied parallel to the conduction plane. However, the superconducting states of the conventional κ-type salts are usually almost isotropic in the conduction plane. On the other hand, in the κ-$(BETS)_2FeBr_4$ salt, the situation is quite complex due to the existence of the antiferromagnetic ordering and metamagnetic behavior of the Fe^{3+} localized internal spin system. When one applies the magnetic fields along the easy axis of the antiferromagnetic transition ($H \parallel a$), the superconducting transition is gradually suppressed to 1.0 T, then almost broken suddenly at 1.6 T. On the other hand, the application of the magnetic fields along the hard axis ($H \parallel c$) makes a quicker suppression of the superconducting state than in the case applied along the easy axis. This anisotropic behavior of the magnetic field dependence of the superconducting state in the conduction plane is considered to originate from the difference of the internal magnetic fields produced by the magnetization of the Fe^{3+} d-spins of the anion layers that is anisotropically induced by the applied magnetic fields (see section 6).

4. Specific Heat Measurements of κ-$(BETS)_2FeBr_4$

The κ-$(BETS)_2FeBr_4$ salt shows the transition from the antiferromagnetic metal phase to the superconducting phase. It is of considerable interest to investigate whether the antiferromagnetic spin ordering and superconductivity coexist below the Néel temperature. To confirm the bulk nature of the phase transitions and to inquire into the possibility of the coexistence of the spin ordering and the superconductivity at low-temperatures, we performed specific heat measurements by the thermal relaxation method using a ^{3}He cryostat down to about 0.9 K.[30b] The temperature dependence of the specific heat (C_p) of the κ-$(BETS)_2FeBr_4$ salt is shown in Fig. 8. In Fig. 8, the zero-field specific heat shows a large anomaly characterized by a sharp λ-type peak at 2.5 K, which corresponds to the antiferromagnetic transition temperature detected by the magnetic susceptibility measurements. The integration of C_p/T vs T curve with respect to temperature gives the information on the entropy [$S(T)$] distribution around the peak, as shown in Fig. 9. The value of the entropy [$S(T)$] reaches to $R\ln 6$ ($=R\ln(2S+1) = 14.9\ \mathrm{J\,mol^{-1}\,K^{-1}}$ for $S = 5/2$) at about 3.8 K, corresponding to the full entropy that comes from the magnetic specific heat based on the degenerate freedom of $S = 5/2$ spins, although we cannot exclude some additional entropy coming from the lattice specific heat that becomes gradually larger as the temperature increases. By applying magnetic fields perpendicular to the *ac*-plane, one finds that the peak position shifts to lower temperatures of 2.36 K at

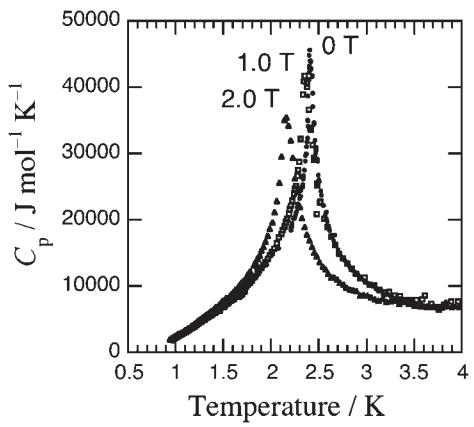

Fig. 8. Temperature dependence of specific heats (C_p) of κ-$(BETS)_2FeBr_4$ measured under zero-field (closed circles), 1.0 T (opened squares), and 2.0 T (closed triangles) at 0.9–4 K.

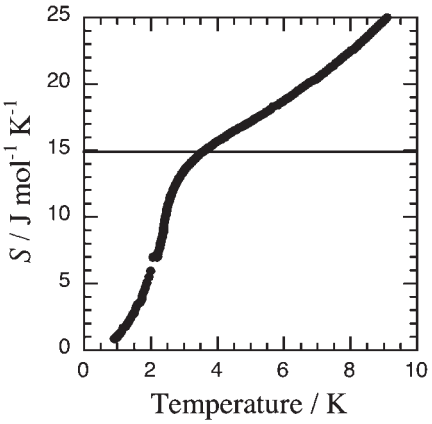

Fig. 9. Temperature dependence of entropy distribution (S) around the peak of the antiferromagnetic transition at $T_N = 2.5$ K. The thin line indicates the full entropy ($14.9\ J\,mol^{-1}\,K^{-1}$) calculated for $S = 5/2$ system.

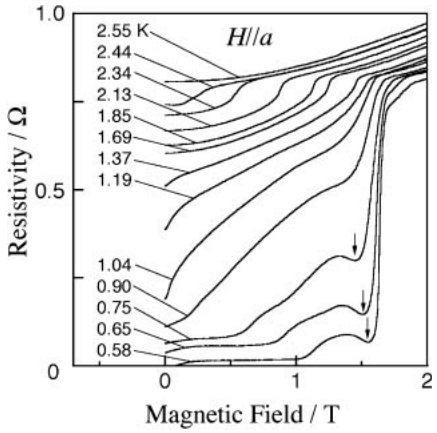

Fig. 10. Magnetic field dependence of magnetoresistances up to 2 T at the indicated temperatures in the figure with an application of the magnetic field in parallel with the a-axis.

1.0 T and 2.05 K at 2.0 T, respectively. These results imply that the observed magnetic ordering is surely an antiferromagnetic one and that the spin state of the Fe^{3+} ions is an $S = 5/2$ high-spin state. In addition, we cannot observe any anomaly around the superconducting transition temperature (1.1 K), which demonstrates that the antiferromagnetically ordered state is not destroyed by the appearance of another phase transition, namely the superconductive transition in the π-conduction layers. Therefore, the antiferromagnetic ordering and the superconductivity coexist at low temperatures below $T_c =$ 1.1 K. This is the first organic salt in which the long range magnetic ordering of the magnetic anions mediated by π-electron donor molecules and the superconductivity based on the π-conduction electrons in the donor layers coexist in a hybrid structure composed of the antiferromagnetic insulator and superconductor layers.

5. Switching of Conducting Properties by the Combination of the Metamagnetism and Superconductivity

For the practical realization of molecular electronic devices, it is essential to develop the "dual-action system" whose conducting properties can be sharply controlled by external forces. A possible candidate for the dual-action system is a hybrid system consisting of the organic layers responsible for electrical conductivities and the inorganic layers with localized magnetic moments, where the conductivity can be controlled by tuning the magnetic states of the inorganic layers. To investigate the field dependence of resistivities and to examine a possibility of switching of conducting properties, the electrical resistivities of κ-$(BETS)_2FeBr_4$ were measured parallel to the a-axis by a four-probe technique.[31] The axis of the crystal was carefully oriented to the applied magnetic field because the magnetic field-induced phenomena like field-induced superconductivity are very sensitive to the inclination of the applied fields from the conduction plane due to an orbital effect which destroys superconductivities.

The resistivity measurements were performed up to 2.0 T to confirm the field-induced transition between the antiferromagnetic superconducting state and the forced-ferromagnetic metal state. As shown in Fig. 10, the resistivity suddenly increases at

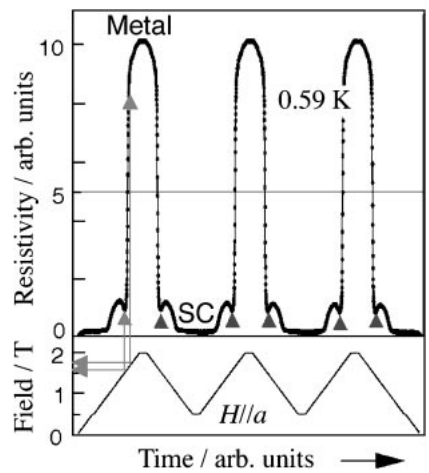

Fig. 11. Switching behavior of κ-$(BETS)_2FeBr_4$. The periodic superconductor–metal switching synchronizing with the periodical modulation of the applied magnetic field ($H \parallel a$) around 1.6 T at 0.59 K.

about 1.6 T with an increase of the applied magnetic field applied parallel to the a-axis ($\parallel$ easy axis) at 0.58 K, and the system recovers its metallic state. This field of the destruction of the superconducting state just corresponds to the metamagnetic transition field of the Fe^{3+} spin system. These results suggest that the internal field that originates from the π–d coupling between the π electrons and the ferromagnetically aligned Fe^{3+} spins, which is sharply induced at 1.6 T, destroys abruptly the superconducting state. Therefore, this phenomenon is considered to originate from the bi-functionality of the π–d coupled magnetic organic superconductor κ-$(BETS)_2FeBr_4$, where an unprecedented combination of metamagnetism and superconductivity is realized. To investigate the switching functionality of electrical resistivities, we measured the resistivity of κ-$(BETS)_2FeBr_4$ at 0.59 K while periodically changing external fields around 1.6 T. We found that the superconducting state can be sharply switched on or off by controlling the metamagnetism of the anion layers by external fields (Fig. 11).

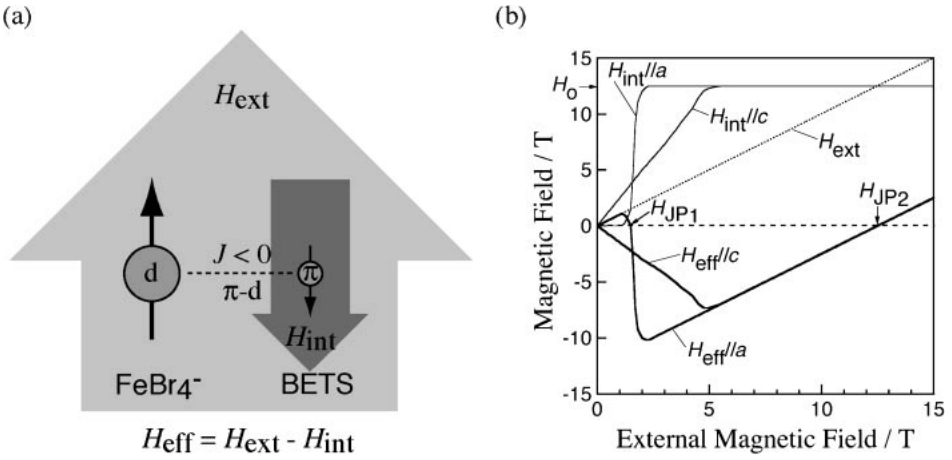

Fig. 12. (a) Schematic drawing of the Jaccarino–Peter compensation effect. (b) Schematic plot of the applied external magnetic field (H_{ext}) dependence of the induced internal field (H_{int}) by the Fe^{3+} spin system and the effective field (H_{eff}) on the BETS layers, which is obtained as $H_{eff} = H_{ext} - H_{int}$. The suffix $\| a$ and $\| c$ denote that the external field (H_{ext}) was applied parallel to the a-axis and c-axis, respectively. The dotted line: H_{ext}; thin lines: H_{int}; thick lines: H_{eff}. H_o is the internal field from the fully magnetized Fe^{3+} spin system. H_{JP1} and H_{JP2} indicate the fields for the Jaccarino–Peter compensation effect.

6. Magnetic Field-Induced Superconductivities in κ-$(BETS)_2FeBr_4$

In general, superconductivities are destroyed by applied magnetic fields. However, Uji et al. discovered a magnetic field-induced superconductivity (FISC) under very high magnetic fields ($18\ T < H < 41\ T$) in the λ-$(BETS)_2FeCl_4$ salt in 2001;[25] this is considered to be caused by the Jaccarino–Peter compensation effect.[40] Figure 12a shows a schematic drawing of the Jaccarino–Peter compensation effect. When the magnetic field (H_{ext}) is applied, the Fe^{3+} spin system has a magnetization corresponding to the strength of the applied field; H_{ext} causes a negative internal field (H_{int}) on the conduction layer by a negative exchange interaction ($J < 0$) through the π–d interaction. Then, if such a negative internal field caused by the Fe^{3+} spin and a positive external field are cancelled out, the effective magnetic field (H_{eff}) becomes zero and FISC can appear because of the suppression of a Zeeman effect that destroys superconductivities under applied magnetic fields.

In the field dependence of magnetoresistances when the field is applied parallel to the a-axis, a conspicuous resistivity decrease was observed just below the abrupt resistivity increase at 1.6 T, as shown in Fig. 10. As mentioned before, the superconducting state is broken by the sudden appearance of the metamagnetically induced internal field. Namely, such an internal field created by the Fe^{3+} spins is considered to produce a negative magnetic field on the π-electron system through the antiferromagnetic exchange coupling between the d and π electron systems. Then, around the onset field of the metamagnetic transition, there should be a magnetic field where the applied external field (H_{ext}) is balanced with the rapidly growing internal field (H_{int}). At this point, the superconductivity tends to be stabilized because of a reduced effective field on the π electron system (H_{eff}). Thus, the resistivity minimum around 1.6 T suggests the compensation of H_{ext} by H_{int}. Figure 12b illustrates the relationship between H_{eff} ($=H_{ext} - H_{int}$) and H_{ext}. Here we assumed H_{int} to be proportional to the magnetization of the Fe^{3+} spins that shows the metamagnetic transition, as shown by the thin lines in Fig. 12b. When applying the external magnetic field parallel to the easy axis ($H \| a$), the sign of $H_{eff} \| a$ is considered to be changed from positive to negative at 1.6 T (H_{JP1}) and then to return to positive at the field ($H_{JP2} = H_o$) corresponding to the internal field (H_o) produced by the fully magnetized Fe^{3+} spin system. Consequently, there should be two zero-field points at H_{JP1} and H_{JP2} ($H_{eff} = 0$). Therefore, it may be possible to discover another FISC state around H_o if T_c of this superconducting state is not too low to be detected. On the other hand, on the application of the magnetic field parallel to the hard axis ($H \| c$), initial effective fields are already negative because of a large magnetization of Fe^{3+} spins, and only one compensation point will be expected at the same compensation field of H_{JP2} ($=H_o$), as shown in Fig. 12b.

In order to confirm the possibility of this FISC, we performed further investigations of magnetoresistances under the magnetic fields up to 15 T applied along the a axis ($H \| a$) and c axis ($H \| c$) at the temperatures indicated in Fig. 13. In contrast to the case of $H \| a$, where the sharp "antiferromagnetic superconductor-to-ferromagnetic metal transition" is observed around 1.6 T (H_{JP1}), only gradual breaking of the superconducting state is observed for $H \| c$. Needless to say, this anisotropic resistivity behavior comes from the interplay between the magnetic ordering and superconductivity. When the magnetic field is increased up to 15 T, further anomalies are observed at the field range of 10–15 T below 0.75 K for both magnetic fields $H \| a$ and $H \| c$, as shown in Fig. 13. Although the lowest experimental temperatures are not sufficiently low, the resistivity changes between 1.19 K (the normal state) and the lowest measured temperatures [0.58 K ($H \| a$), 0.60 K ($H \| c$)] plotted in the insets strongly suggest the onset of FISC around 12.5 T ($= H_{JP2}$).

Very recently Konoike et al. examined the magnetoresistances down to lower temperature of 27 mK using a dilution refrigerator and a sample rotator that enables a setting of the crystal exactly parallel to the magnetic fields to confirm zero

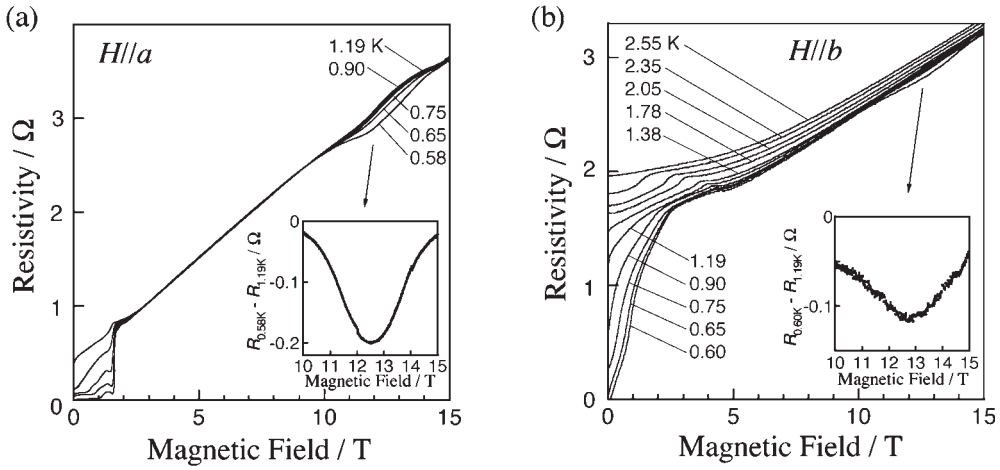

Fig. 13. Magnetic field dependence of magnetoresistances up to 15 T at the indicated temperatures in the figures with an application of the magnetic field in parallel with (a) the *a*-axis and (b) the *c*-axis. The insets show the resistivity differences between the data at 1.19 K and one at the lowest measured temperature [(a) 0.58 K (b) 0.60 K].

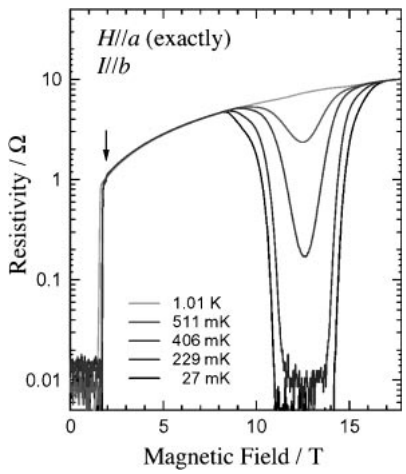

Fig. 14. Magnetic field dependence of resistivities at the indicated several temperatures under the magnetic field exactly parallel to the *a*-axis up to 17.5 T (From Ref. 41).

resistivities in the FISC state.[41] Measurements were performed under high magnetic fields up to 17.5 T with electrical currents perpendicular to the conduction plane ($I \parallel b$). Figure 14 shows the field dependence of resistivities at various temperatures for the magnetic fields exactly parallel to the *a*-axis. As the magnetic field increases, the superconductivity is broken at about 1.8 T, followed by a step-like increase indicated by an arrow. At 27 mK, the resistivity increases almost linearly above 2 T, and then shows a steep drop above 8 T. In the field region of about 11–14 T, the resistivity becomes almost zero within the instrumental resolution (below noise level). This behavior strongly suggests the FISC state in this salt. At higher fields above 16 T, this state seems to be completely removed. As the temperature increases, the field region of the FISC phase becomes narrower and the FISC state is almost completely suppressed at 1 K.

This field of the FISC just corresponds to the field (12 T) theoretically predicted by Cépas et al. on the basis of the splitting of Shubnikov–de Haas (SdH) frequencies.[42] In the previous SdH oscillation measurements in κ-$(BETS)_2FeBr_4$, two peaks in the Fourier transform spectrum, which arise from the magnetic breakdown β orbit, were observed as shown in Fig. 3.[39b] In the presence of a large internal field, it is expected that two frequencies corresponding to the two Fermi surfaces of the up and down spin electrons will be observed. The internal field can be directly calculated from the difference of the frequencies, $\Delta F = (1/4)g \times (m_{\text{eff}}/m_0) \times H_J$, where m_{eff} is the effective mass ($=7.9m_0$) and g is the g-factor. Assuming $g = 2$, we obtain the internal field of 12.7 T. This value is in quite good agreement with the center field of the FISC region. Therefore, we conclude that this FISC is induced by the Jaccarino–Peter compensation mechanism as in the case of λ-$(BETS)_2FeCl_4$.[25] From the discovery of the FISC in κ-$(BETS)_2FeBr_4$, it is undoubted that the FISC is a universal phenomenon if the conditions: i) low dimensionality, ii) presence of the large localized magnetic moments, and iii) strong negative exchange interaction J between the conduction electrons and magnetic moments, are satisfied.

The critical field of this FISC state ($H_{JP2} = 12.5$ T) is about one-third of that of the first magnetic field-induced organic superconductor λ-$(BETS)_2FeCl_4$ ($H_{JP} = 33$ T). These two salts have several similarities: they have the layered structure consisting of the two-dimensional conduction layers and they have the insulating layers involving the magnetic iron atoms that show the antiferromagnetic transition at low temperatures. But their ground states are quite different. In the λ-$(BETS)_2FeCl_4$ salt, the strong π–d coupling suggested from strong contacts between chlorine and selenium atoms results in the cooperative transition to the antiferromagnetic insulating state at T_N. On the other hand, such short intermolecular contacts were not observed in κ-$(BETS)_2FeBr_4$ and consequently the metallic state could be maintained during the antiferromagnetic transition of the anion layers and thus the antiferromagnetic superconducting state is realized. Estimation of the π–d interaction in the λ-$(BETS)_2FeCl_4$ and κ-$(BETS)_2FeBr_4$ salts was examined by T. Mori et al. using a mean-field approximation based on intermolecular overlap integrals. Their results suggested that the π–d interaction of κ-$(BETS)_2FeBr_4$ is quite small in comparison with that of λ-$(BETS)_2FeCl_4$.[43] There-

fore, the induced internal magnetic field on the BETS layers in κ-$(BETS)_2FeBr_4$ is considered to be weaker than that in λ-$(BETS)_2FeCl_4$, which is consistent with the smaller compensation field of κ-$(BETS)_2FeBr_4$. However, for $H \parallel a$, the situation of κ-$(BETS)_2FeBr_4$ is more complicated because of the existence of the metamagnetic transition which makes this system a "dual-functional" material and gives rise to the field-induced resistivity decreases suggesting the stabilization of the superconducting states at two characteristic magnetic fields of 1.6 T and 12.5 T.

7. Thermal Conductivity of κ-$(BETS)_2FeBr_4$ under Magnetic Fields

While the antiferromagnetic transition was confirmed by the specific heat measurements, no specific heat anomaly was found at T_c. Characterization of the superconducting state in this material is still quite important. Tanatar et al. recently reported the results on the thermal conductivity and electrical resistivity measurements of κ-$(BETS)_2FeBr_4$ in magnetic fields applied parallel to the conduction plane.[44] The contacts to the crystals were made by Au evaporation on the top and side surfaces of the sample and by gluing Pt wires with Ag contact paste. This procedure provided contact resistance values of 0.1 to 0.5 Ω. Measurements of thermal conductivity were performed with heat current along the *a*-axis in the conduction plane by a standard steady-state one-heater-two thermometers technique in a miniature rotatable vacuum cell, as described elsewhere.[45]

Figure 15 shows the temperature dependence of the thermal conductivity together with that of the electrical resistivity below 3 K. A clear change is seen in both curves at T_N. It indicates that the magnetic moments of the Fe^{3+} ions are not completely isolated from the conduction band formed by the HOMO orbitals of BETS molecules, and that there is a notable π–d interaction. It is noteworthy that the superconducting transition does not give a sharp anomaly in $\kappa(T)$ at T_c, while at 0.14 K, the base temperature of our experiment, the difference between the normal and superconducting states accounts for 70% of the electronic conductivity in the normal state estimated from the Wiedemann–Franz law. This clearly shows that the main superconducting state is bulk in nature.

The field dependence of κ and ρ up to 17 T for $H \parallel c$ is shown in Fig. 16. The transition from the main superconducting phase into the normal metallic state is gradual and looks 2nd order in this direction. On H increase above H_{c2}, both ρ and κ show a tiny anomaly at 4 T, which corresponds to a metamagnetic transition field for this field direction; then both ρ and κ show a shallow dip in the field range of ca. 10 to 15 T. In terms of the Wiedemann–Franz law, $\kappa/\rho =$ constant at a constant temperature, a decrease of electrical resistivity in the normal state should lead to an increase of thermal conductivity. This simultaneous decrease in κ and ρ in our observation strongly indicates the system is really in a new superconducting state. A clear change of the thermal conductivity in both superconducting states provides some evidence for the bulk origin of superconductivity, coexisting with the magnetic order in both main and reentrant states.

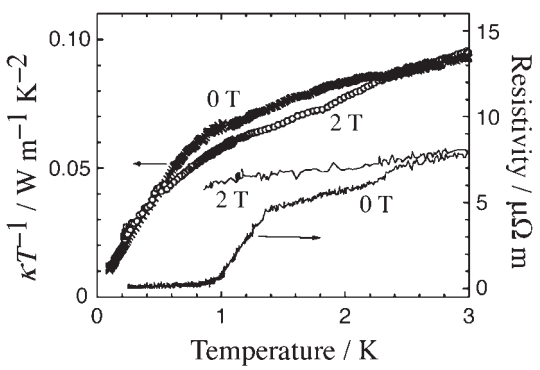

Fig. 15. Temperature dependence of thermal conductivities (κ) and electrical resistivities (ρ) below 3 K under 0 and 2 T (From Ref. 44).

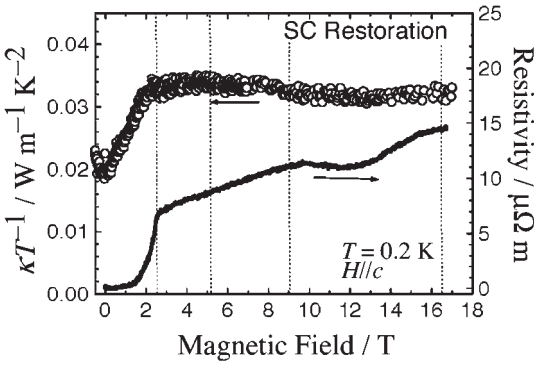

Fig. 16. Field dependence of thermal conductivities (κ) and electrical resistivities (ρ) up to 17 T for the orientation of magnetic field parallel to the *c*-axis at 0.2 K (From Ref. 44).

8. Physical Properties of the κ-$(BETS)_2FeBr_xCl_{4-x}$ ($0 \le x \le 4$) Alloy System

The specific heat measurements of κ-$(BETS)_2FeBr_4$ showed that the Fe^{3+} spins undergo a transition from paramagnetic state to three-dimensionally ordered state around 2.5 K, while the transition entropy of κ-$(BETS)_2FeCl_4$ suggested the low-dimensional nature of the Fe^{3+} spin system.[46b] In contrast to the λ-type salt, where the crystals of λ-$(BETS)_2MBr_xCl_{4-x}$ (M = Fe and Ga) can be obtained only for a small *x*-range ($x < 1.0$),[47] Br and Cl atoms are exchanged freely in the κ-type alloy system, κ-$(BETS)_2FeBr_xCl_{4-x}$ ($0 \le x \le 4$). Therefore, the magnetic and superconducting properties of the κ-type salt can be modified continuously over a wide range of the *x*-value. Then, we examined the electrical and magnetic properties of the κ-$(BETS)_2FeBr_xCl_{4-x}$ alloy system to study the "chemical pressure effect" on the physical properties.[32]

Plate crystals of κ-$(BETS)_2FeBr_xCl_{4-x}$ ($0 \le x \le 4$) were obtained electrochemically using mixed supporting electrolytes of $[(C_2H_5)_4N]FeBr_4$ and $[(C_2H_5)_4N]FeCl_4$ with a suitable mixing ratio. The Br content (*x*) were estimated by the unit cell volume of the crystals (*V*), which can be fitted by the linear relation: V (Å^3) $= 3557 + 28x$. The lattice constants, *a* and *c* are only slightly dependent on *x*; however, the *b*-axis becomes shorter with the increase of the Cl content, suggesting that the thickness of the anion layer changes remarkably by the substitution of the halogen atoms. It is interesting that, despite the large difference in the temperature dependence of resistivities between $FeBr_4^-$ and $FeCl_4^-$ salts, only a slight

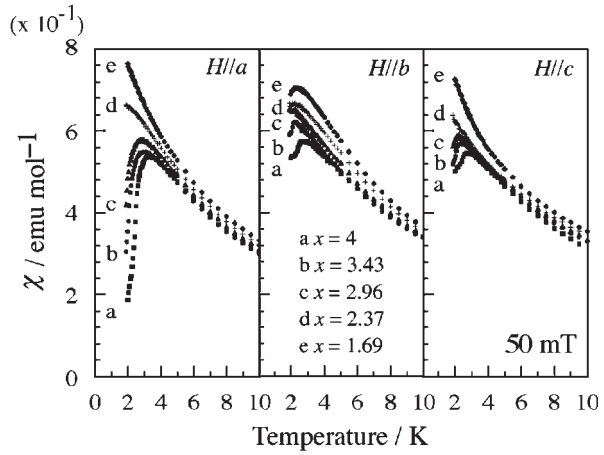

Fig. 17. Temperature dependences of magnetic susceptibilities (χ) of single crystals of κ-(BETS)$_2$FeBr$_x$Cl$_{4-x}$ for the field (50 mT) parallel to the *a*-, *b*-, and *c*-axes. a: $x = 4$, b: $x = 3.43$, c: $x = 2.96$, d: $x = 2.37$, and e: $x = 1.69$.

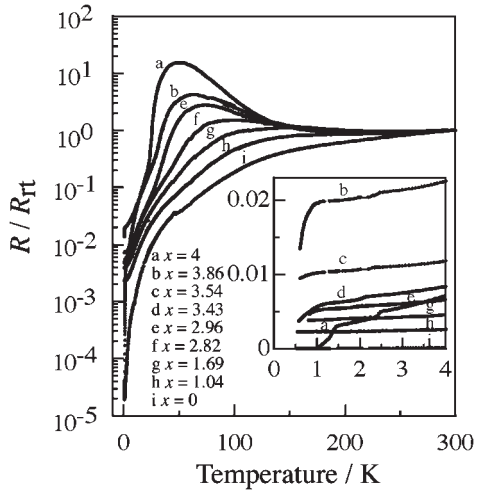

Fig. 18. Temperature dependences of normalized electrical resistivities (R/R_{rt}) of κ-(BETS)$_2$FeBr$_x$Cl$_{4-x}$. a: $x = 4$, b: $x = 3.86$, c: $x = 3.54$, d: $x = 3.43$, e: $x = 2.96$, f: $x = 2.82$, g: $x = 1.69$, h: $x = 1.04$, and i: $x = 0$. The inset shows the resistivity behavior at low temperature region below 4 K.

structural change occurs in the conduction layer (namely, in the *ac* plane).

Magnetic susceptibility measurements were carried out at the field of 50 mT applied parallel to the *a*-, *b*-, and *c*-axes. The temperature dependences of magnetic susceptibilities of κ-(BETS)$_2$FeBr$_x$Cl$_{4-x}$ ($x = 4$, 3.43, 2.96, 2.37, and 1.69) are shown in Fig. 17. The sharp susceptibility decrease corresponding to the antiferromagnetic transition becomes inconspicuous with decreasing x from $x = 4$, and is hardly observable above 2 K for the field parallel to the *a*-axis in the sample of $x = 2.37$. However, the susceptibility decreases are observed in the samples of $x = 2.37$ and 1.69 only for the field parallel to the *b*-axis. These results suggest that the easy axis of the antiferromagnetic ordering tends to move from the *a*-axis to the *b*-axis with increasing the Cl content. Similar rotation of the easy axis of spin structure by the halogen exchange has been observed in the antiferromagnetic insulating state of λ-(BETS)$_2$FeBr$_x$Cl$_{4-x}$.[47b] The antiferromagnetic transition temperature (T_N) is decreased with decreasing x and is observed at 0.45 K for κ-(BETS)$_2$FeCl$_4$.[46] These results indicate that the magnetic interaction between the Fe^{3+} spins in κ-(BETS)$_2$FeBr$_x$Cl$_{4-x}$ becomes weaker with increasing the Cl content, regardless of the decrease of the thickness of the anion layer. It seems that the relatively small energy differences between 3d orbitals of Fe and 4p orbitals of Br atoms compared with 3p orbitals of Cl atoms, which will increase the "d–p mixing", and the large electron cloud of the Br atom will contribute to enhance the intermolecular magnetic interaction through the halogen atoms.[43] Therefore, the antiferromagnetic interaction between the adjacent FeX_4^- (X = Br, Cl) anions through the X···X and X···S (or Se) contacts will be reduced with increasing the Cl content.

The electrical resistivities were measured down to 0.65 K along the conduction plane (the *ac*-plane). Temperature dependences of normalized electrical resistivities of κ-(BETS)$_2$FeBr$_x$Cl$_{4-x}$ ($x = 4$, 3.86, 3.54, 3.43, 2.96, 2.82, 1.69, 1.04, and 0) are shown in Fig. 18. The maximum of resistivities around 50 K observed in κ-(BETS)$_2$FeBr$_4$, indicating the strong correlation of π-conduction electrons, is suppressed with the increase of Cl content as if the crystals are subject to pressures [so-called "chemical pressure effect" associated with the halogen exchange as observed in λ-(BETS)$_2$MBr$_x$Cl$_{4-x}$ (M = Fe and Ga) alloy system][47] and almost disappears in the sample of $x = 1.69$. The role of Fe^{3+} moments will not be essential for this systematic change of the resistivity behavior, because a similar difference of the resistivity behavior has been observed also in κ-(BETS)$_2$GaX$_4$ (X = Br, Cl).[21] On the other hand, the electrical resistivities at low temperatures are decreased with the increase of the Cl content. As shown in the inset of Fig. 18, the onset temperature of superconducting transition determined from the resistivity decrease shifts to lower temperatures with increasing the Cl content. For example, T_c(onset) is 1.2 K for the sample with $x = 3.86$ and that of κ-(BETS)$_2$FeBr$_4$ is 1.45 K. In the case of κ-(BETS)$_2$FeBr$_{2.96}$Cl$_{1.04}$, a slight decrease of electrical resistivities is still observed below 0.85 K. Therefore, the Br/Cl disorder in the anion sites seems unimportant in the superconducting transition of κ-(BETS)$_2$FeBr$_x$Cl$_{4-x}$. The step-like resistivity decrease, corresponding to the antiferromagnetic transition, is observed at 2.5 K–1.4 K for the sample with $x = 4$–1.69.

The temperature vs x-value phase diagram of κ-(BETS)$_2$FeBr$_x$Cl$_{4-x}$ ($0 \leq x \leq 4$) was obtained by summarizing the experimental results on the electrical resistivities and magnetic susceptibilities (Fig. 19). The paramagnetic metallic phase exists around room temperature. The paramagnetic nonmetallic phase appears around 50–250 K for the samples of $x \geq 1.69$ and is suppressed gradually with the increase of Cl content. Moreover, the antiferromagnetic metallic phase is observed below 2.5 K, but T_N is lowered with increasing the Cl content. The antiferromagnetic superconducting phase exists in the lowest temperature region, but the superconducting transition is difficult to observe for the samples of $x \leq 2.96$ in the present experiments. Since there is no other molecular conductor like κ-(BETS)$_2$FeBr$_x$Cl$_{4-x}$ exhibiting successive antiferromagnetic

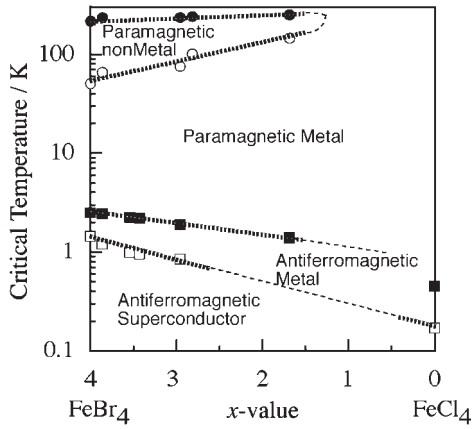

Fig. 19. Temperature vs x-value phase diagram of κ-$(BETS)_2FeBr_xCl_{4-x}$. The filled circles: the temperatures of resistivity minimum around room temperature; opened circles: the temperatures of maximum of resistivities; filled squares: the Néel temperatures (T_N); and opened squares: the superconducting transition temperatures (T_c). For κ-$(BETS)_2FeCl_4$, the reported data of T_N and T_c are adopted (Refs. 46 and 48).

and superconducting transitions, this phase diagram is the first diagram showing the relationship between the magnetic and superconducting transition temperatures in the molecular systems. Though both $\log(T_N)$ and $\log(T_c)$ seem to decrease approximately linearly with increasing the Cl content, their x-dependences are not wholly identical to each other. The $\log(T_c)$ vs x line seems to be connected smoothly with the datum point of T_c of κ-$(BETS)_2FeCl_4$ ($T_c = 0.17$ K)[48] but the antiferromagnetic transition temperature of the $FeCl_4^-$ salt ($T_N = 0.45$ K)[46,48] is somewhat lower than the temperature expected from the x-dependence of T_N obtained for $x > 1.69$. This discrepancy seems to be related to the low-dimensionality of the Fe^{3+} spin system of the $FeCl_4^-$ salt.[46]

9. Hydrostatic Pressure Dependence of Electrical Resistivities of κ-$(BETS)_2FeBr_4$

For the purpose of further understanding of the π–d interaction in κ-$(BETS)_2FeBr_4$, we measured electrical resistivities under high pressure by use of a clamp-type pressure cell made of Be/Cu alloy and Daphne 7373 oil (Idemitsu Company) as a pressure medium.[33] As shown in Fig. 20, the characteristic broad maximum around 50 K observed under atmospheric pressure is suppressed by applying pressure and disappears around 2.5 kbar; above 3.5 kbar the resistivity shows a monotonic decrease down to low temperatures. As discussed above, the prominent broad peak is considered to be a sign of the strong correlation of π conduction electrons. Thus, the suppression of the broad resistivity peak of κ-$(BETS)_2FeBr_4$ at high pressure suggests the enhancement of the intermolecular transfer integral between the BETS dimers. The same suppression of resistivity peak was also realized by the chemical pressure effect in the alloy system κ-$(BETS)_2FeBr_xCl_{4-x}$ ($0 < x < 4$), as discussed in section 7.

In the κ-$(BETS)_2FeBr_xCl_{4-x}$ ($0 < x < 4$) alloy system, the Néel temperature T_N and the superconducting transition temperature T_c decrease as the content of bromine (x) decreases,

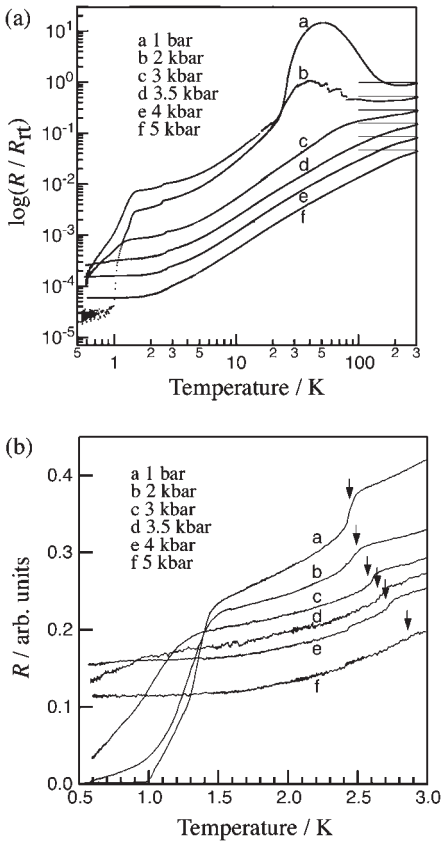

Fig. 20. (a) Temperature dependence of normalized resistivities (R/R_{rt}) of κ-$(BETS)_2FeBr_4$ at high pressure (<5 kbar): a, 1 bar (ambient); b, 2 kbar; c, 3 kbar; d, 3.5 kbar; e, 4 kbar; f, 5 kbar. (b) The expansion of the low-temperature region below 3 K.

in other words, as the chemical pressure increases. Therefore, if the real pressure gives the same effect on the resistivities as the chemical pressure, both T_N and T_c will decrease by applying pressures. Similar to most of the other organic superconductors, T_c of κ-$(BETS)_2FeBr_4$ is reduced by applying pressure.[3] The T_c value of κ-$(BETS)_2FeBr_4$ becomes less than 0.5 K around 4 kbar. However, as shown in Fig. 20b, although T_c of κ-$(BETS)_2FeBr_4$ decreases with increasing applied real pressure, T_N increases as the real pressure increases. Figure 21 shows the pressure–temperature phase diagram of κ-$(BETS)_2FeBr_4$.

Thus, the real pressure affects the magnetic properties contrary to the chemical pressure. In terms of the halogen replacement from bromine to chlorine atom in κ-$(BETS)_2FeBr_xCl_{4-x}$,[32] both the direct d–d interaction between the anions and the π–d interaction between the donor and anion will be strongly reduced, regardless of the decrease of the thickness of anion layer. On the other hand, both the intermolecular d–d and π–d interactions will increase with increasing the real pressure, which will result in the enhancement of the magnetic transition temperature.

Concluding Remarks

The κ-$(BETS)_2FeBr_4$ salt is the first organic salt in which the long range antiferromagnetic ordering ($T_N = 2.5$ K) of

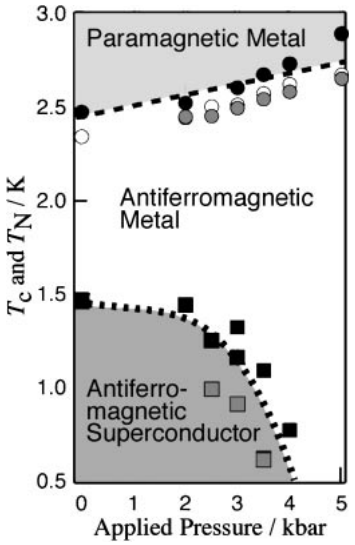

Fig. 21. (a) Pressure–temperature phase diagram of κ-$(BETS)_2FeBr_4$. The circles and squares denote the Néel temperatures T_N and critical temperatures T_c, respectively (white and grey: $I \parallel a$; black: $I \parallel b$).

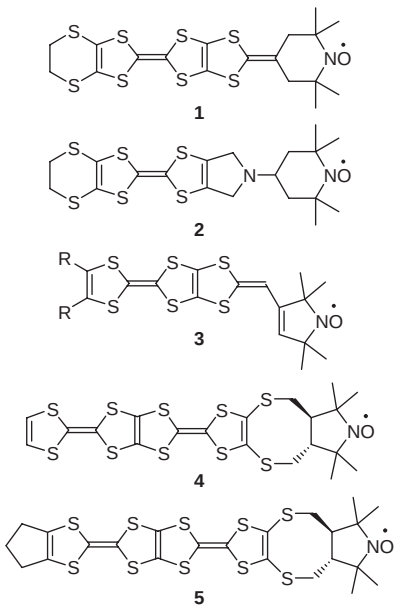

Chart 3.

the Fe^{3+} localized spins and the superconductivity ($T_c = 1.1$ K) based on the π-conduction electrons in the donor layers coexist in the hybrid structure composed of the antiferromagnetic insulator and superconductor layers. This coexistence had been observed in the inorganic ternary systems like as the rhodium–boride phase, $RERh_4B_4$ (RE = Nd, Sm) and the Chevrel compounds, $REMo_6S_8$ (RE = Gd, Tb, Dy, and Er) in which the 4d electrons of Rh or Mo atoms show superconductivity and the 4f spins of rare earth atoms order antiferromagnetically below T_c.[49,50] However, except the κ-$(BETS)_2FeBr_4$ salt, the phase transition from the antiferromagnetic metal phase to the antiferromagnetic superconducting phase had been observed in only the $Ho(Ir_xRh_{1-x})_4B_4$ ($x \geq 0.6$) system.[51] The magnetic field dependence of magnetoresistances suggests that the superconductivity in this system has a remarkable anisotropy in the conduction plane because of the metamagnetism of the Fe^{3+} localized spin system, in contrast to the cases of the other conventional organic superconductors. Furthermore, we discovered two characteristic field-induced superconducting regions around 1.6 T and 12.5 T that are caused by the combination of the metamagnetism and superconductivity in terms of the Jaccarino–Peter compensation effect. This means κ-$(BETS)_2FeBr_4$ is the π–d interacted dual-functional organic superconductor in which the superconducting state can be controlled by the magnetic state of the internal magnetic d-spin system. We investigated the chemical pressure effect by a halogen exchange in the alloy system κ-$(BETS)_2FeBr_xCl_{4-x}$ and the physical pressure effect by an application of real pressures in κ-$(BETS)_2FeBr_4$, and showed that the π–d interaction and the d–p mixing of anion molecules in the κ-$(BETS)_2FeBr_4$ system play important roles in the appearance of the antiferromagnetic long-range ordering.

As one of different approaches to the magnetic molecular conductors, several attempts have been performed to achieve the synthesis of donor and acceptor molecules to which stable radical parts are directly connected for the realization of the strong interaction between π-conduction electrons of the conducting part and localized spins of the organic stable radical parts.[52] However, the large steric hindrance of stable radical parts had made it difficult to construct enough conduction pathways necessary for highly conducting cation radical salts so far. To overcome these problems, we focused on the π-extended donor skeletons, which are effective for establishing sufficient intermolecular overlap integrals and π-conduction bands. We reported several π-extended donor molecules that contain a stable organic radical part (**1**–**5**) (Chart 3),[53,54] and discovered highly conducting cation radical salts using a bis-fused TTF skeleton called as "TTP"[55] that contains PROXYL radical substituent **4**.[54]

Very recently, we successfully determined the first crystal structure of a cation radical salt based on a TTP derivative, $(\mathbf{5})_4AsF_6$.[56] In this salt, the TTP skeletons of the donor molecules form π-conduction layers that show a relatively high room temperature conductivity of about 1 S cm^{-1}. The radical parts and the AsF_6^- anions form insulating layers sandwiched between the π-conduction layers. Furthermore, magnetic properties of this salt suggest the coexistence of the conduction electron and the localized spin in a molecule around room temperatures. These conditions will allow pure organic magnetic conductors to be constructed in the near future. These fundamental studies on the bifunctionality of organic conductors are a useful first step for realizing future nano-scaled functional molecular electronic devices.

The author (H. F.) wishes to thank Dr. Emiko Fujiwara for her collaboration, supports, understanding, and continuous encouragement. The authors are deeply grateful to all the collaborators whose names appeared in co-authored published papers. This work was financially supported by Grants-in-Aid for Scientific Research on Priority Areas (B) of Molecular Conductors and Magnets (Nos. 11224101 and 11224211) from the Ministry of Education, Culture, Sport, Science and Technology, Japan. This work is also supported by CREST (Core

Research for Evolutional Science and Technology) of JST (Japan Science and Technology Agency).

References

1 a) J. Ferraris, D. O. Cowan, V. V. Walatka, and J. H. Perlstein, *J. Am. Chem. Soc.*, **95**, 948 (1973). b) L. B. Coleman, J. A. Cohen, D. J. Sandman, F. G. Yamagishi, A. F. Garito, and A. J. Heeger, *Solid State Commun.*, **12**, 1125 (1973).

2 a) "TTF Chemistry," ed by J. Yamada and T. Sugimoto, Kodansha Ltd., Tokyo, and Springer-Verlag Berlin, Heidelberg, New York (2004). b) "Handbook of Organic Conductive Molecules and Polymers," ed by H. S. Nalwa, John Wiley & Sons, Chichester (1997), Vol. 1. c) Recent special issue on "Molecular Conductors," ed by P. Batail, *Chem. Rev.*, **104**, No. 11 (2004).

3 a) T. Ishiguro, K. Yamaji, and G. Saito, "Organic Superconductors," 2nd ed, Springer-Verlag Berlin, Heidelberg (1998). b) J. M. Williams, J. R. Ferraro, R. J. Thorn, K. D. Carlson, U. Geiser, H. H. Wang, A. M. Kini, and M.-H. Whangbo, "Organic Superconductors (Including Fullerenes)," Prentice Hall, New Jersey (1992). c) "Organic Conductors," ed by J.-P. Farges, Marcel Dekker, New York (1994). d) "Studies of High Temperature Superconductors," ed by A. Narlikar, Nova Science Publishers, New York (2000).

4 Reviews: a) M. Narita and C. U. Pittman, Jr., *Synthesis*, **1976**, 489. b) A. Krief, *Tetrahedron*, **42**, 1209 (1986). c) G. Schukat, A. M. Richter, and E. Fanghänel, *Sulfur Rep.*, **7**, 155 (1987). d) M. R. Bryce, *Chem. Soc. Rev.*, **20**, 355 (1991). e) G. Schukat and E. Fanghänel, *Sulfur Rep.*, **14**, 245 (1993). f) N. Svenstrup and J. Becher, *Synthesis*, **1995**, 215. g) J. Garín, *Adv. Heterocycl. Chem.*, **62**, 249 (1995). h) G. Schukat and E. Fanghänel, *Sulfur Rep.*, **18**, 1 (1996). i) T. Otsubo and K. Takimiya, *Bull. Chem. Soc. Jpn.*, **77**, 43 (2004).

5 Reviews: a) D. Jérome and H. J. Schulz, *Adv. Phys.*, **31**, 299 (1982). b) M. R. Bryce and L. C. Murphy, *Nature*, **309**, 119 (1984). c) J. M. Williams, A. J. Schultz, U. Geiser, K. D. Carlson, A. M. Kini, H. H. Wang, W. K. Kwok, M.-H. Whangbo, and J. E. Schirber, *Science*, **252**, 1501 (1991). d) D. Jérome, *Science*, **252**, 1509 (1991). e) A. Underhill, *J. Mater. Chem.*, **2**, 1 (1992). f) J. P. Pouget, *Mol. Cryst. Liq. Cryst.*, **230**, 101 (1993).

6 a) D. Jérome, A. Mazaud, M. Ribault, and K. Bechgaard, *J. Phys. Lett.*, **41**, L95 (1980). b) N. Thorup, G. Rindorf, H. Soling, and K. Bechgaard, *Acta Crystallogr.*, **B37**, 1236 (1981).

7 a) S. S. P. Parkin, E. M. Engler, R. R. Schumaker, R. Lagier, V. Y. Lee, J. C. Scott, and R. N. Greene, *Phys. Rev. Lett.*, **50**, 270 (1983). b) E. B. Yagubskii, I. F. Shchegolev, V. N. Laukhin, P. A. Kononovich, M. V. Karatsovnik, A. V. Zvarykina, and L. I. Buravov, *JETP Lett.*, **39**, 12 (1984).

8 K. Oshima, T. Mori, H. Inokuchi, H. Urayama, H. Yamochi, and G. Saito, *Phys. Rev.*, **B38**, 938 (1988).

9 M. Mizuno, A. F. Garito, and M. P. Cava, *J. Chem. Soc., Chem. Commun.*, **1978**, 18.

10 a) G. Saito, *Phosphorus Sulfur, Silicon*, **67**, 345 (1992). b) H. Yamochi, T. Komatsu, N. Matsukawa, G. Saito, T. Mori, M. Kusunoki, and K. Sakaguchi, *J. Am. Chem. Soc.*, **115**, 11319 (1993).

11 a) T. Mori, *Bull. Chem. Soc. Jpn.*, **71**, 2509 (1998). b) T. Mori, H. Mori, and S. Tanaka, *Bull. Chem. Soc. Jpn.*, **72**, 179 (1999). c) T. Mori, *Bull. Chem. Soc. Jpn.*, **72**, 2011 (1999).

12 A. Kobayashi, R. Kato, H. Kobayashi, S. Moriyama, Y. Nishio, K. Kajita, and W. Sasaki, *Chem. Lett.*, **1987**, 459.

13 a) H. Urayama, H. Yamochi, G. Saito, K. Nozawa, T. Sugano, M. Kinoshita, S. Saito, K. Oshima, A. Kawamoto, and J. Tanaka, *Chem. Lett.*, **1988**, 55. b) H. Urayama, H. Yamochi, G. Saito, S. Sato, A. Kawamoto, J. Tanaka, T. Mori, Y. Maruyama, and H. Inokuchi, *Chem. Lett.*, **1988**, 463.

14 H. Taniguchi, M. Miyashita, K. Uchiyama, K. Satoh, N. Môri, H. Okamoto, K. Miyagawa, K. Kanoda, M. Hedo, and Y. Uwatoko, *J. Phys. Soc. Jpn.*, **72**, 468 (2003).

15 Reviews: a) M. Adam and K. Müllen, *Adv. Mater.*, **6**, 439 (1994). b) T. Jørgensen, T. K. Hansen, and J. Becher, *Chem. Soc. Rev.*, **23**, 41 (1994). c) M. R. Bryce, *J. Mater. Chem.*, **10**, 589 (2000). d) M. B. Nielsen, C. Lomholt, and J. Becher, *Chem. Soc. Rev.*, **29**, 153 (2001). e) J. L. Segura and N. Martín, *Angew. Chem., Int. Ed. Engl.*, **40**, 1372 (2001).

16 Reviews: a) E. Coronado and C. J. Gómez-García, *Comments Inorg. Chem.*, **17**, 255 (1995). b) P. Day and M. Kurmoo, *J. Mater. Chem.*, **7**, 1291 (1997). c) E. Coronado and C. J. Gómez-García, *Chem. Rev.*, **98**, 273 (1998). d) L. Ouahab, *Coord. Chem. Rev.*, **178–180**, 1501 (1998).

17 a) L. I. Buravov, A. V. Gudenko, V. B. Ginodman, A. V. Zvarykina, V. E. Korotkov, N. D. Kushch, L. P. Pozenberg, A. G. Khomenko, R. P. Shibaeva, and E. B. Yagubskii, *Izv. Akad. Nauk SSSP, Ser. Khim.*, **N1**, 206 (1990). b) P. Day, M. Kurmoo, T. Mallah, I. R. Marsden, R. H. Friend, F. L. Pratt, W. Hayes, D. Chasseau, J. Gaultier, G. Bravic, and L. Ducasse, *J. Am. Chem. Soc.*, **114**, 10722 (1992).

18 a) A. W. Graham, M. Kurmoo, and P. Day, *J. Chem. Soc., Chem. Commun.*, **1995**, 2061. b) M. Kurmoo, A. W. Graham, P. Day, S. J. Coles, M. B. Hursthouse, J. L. Caulfield, J. Singleton, F. L. Pratt, W. Hayes, L. Ducasse, and P. Guionneau, *J. Am. Chem. Soc.*, **117**, 12209 (1995). c) L. Martin, S. S. Turner, P. Day, F. E. Mabbs, and E. J. L. McInnes, *Chem. Commun.*, **1997**, 1367.

19 a) E. Coronado, J. R. Galán-Mascarós, C. J. Gómez-García, and V. N. Laukhin, *Nature*, **408**, 447 (2000). b) F. Palacio and J. S. Miller, *Nature*, **408**, 421 (2000).

20 a) R. Kato, H. Kobayashi, and A. Kobayashi, *Synth. Met.*, **41–43**, 2093 (1991). b) A. Kobayashi, R. Kato, T. Naito, and H. Kobayashi, *Synth. Met.*, **55–57**, 2078 (1993).

21 a) A. Kobayashi, T. Udagawa, H. Tomita, T. Naito, and H. Kobayashi, *Chem. Lett.*, **1993**, 2179. b) H. Kobayashi, H. Tomita, T. Naito, A. Kobayashi, F. Sasaki, T. Watanabe, and P. Cassoux, *J. Am. Chem. Soc.*, **118**, 368 (1996).

22 a) H. Kobayashi, A. Kobayashi, and P. Cassoux, *Chem. Soc. Rev.*, **29**, 325 (2000). b) H. Kobayashi, Y. Okano, H. Fujiwara, H. Tanaka, M. Tokumoto, W. Suzuki, E. Fujiwara, and A. Kobayashi, in "Organic Conductors, Superconductors and Magnets: From Synthesis to Molecular Electronics," ed by L. Ouahab and E. B. Yagubskii, Kluwer Academic Publishers, Netherlands (2004), pp. 81–98. c) H. Kobayashi, H.-B. Cui, and A. Kobayashi, *Chem. Rev.*, **104**, 5265 (2004). d) H. Tanaka, H. Kobayashi, A. Kobayashi, and P. Cassoux, *Adv. Mater.*, **12**, 1685 (2000).

23 a) H. Kobayashi, T. Udagawa, H. Tomita, K. Bun, T. Naito, and A. Kobayashi, *Chem. Lett.*, **1993**, 1559. b) H. Kobayashi, H. Akutsu, E. Arai, H. Tanaka, and A. Kobayashi, *Phys. Rev. B*, **56**, R8526 (1997). c) H. Tanaka, A. Kobayashi, A. Sato, H. Akutsu, and H. Kobayashi, *J. Am. Chem. Soc.*, **121**, 760 (1999). d) H. Tanaka, H. Kobayashi, A. Kobayashi, and P. Cassoux, *Adv. Mater.*, **12**, 1685 (2000). e) H. Tanaka, E. Ojima, H. Fujiwara, Y. Nakazawa, H. Kobayashi, and A. Kobayashi, *J. Mater. Chem.*, **10**, 245 (2000).

24 a) H. Akutsu, E. Arai, H. Kobayashi, H. Tanaka, A.

Kobayashi, and P. Cassoux, *J. Am. Chem. Soc.*, **119**, 12681 (1997). b) L. Brossard, R. Clerac, C. Coulon, M. Tokumoto, T. Ziman, D. K. Petrov, V. N. Laukhin, M. J. Naughton, A. Audouard, F. Goze, A. Kobayashi, H. Kobayashi, and P. Cassoux, *Eur. Phys. J.*, **B1**, 439 (1998). c) T. Sasaki, H. Uozaki, S. Endo, and N. Toyota, *Synth. Met.*, **120**, 759 (2001).

25 a) S. Uji, H. Shinagawa, T. Terashima, T. Yakabe, Y. Terai, M. Tokumoto, A. Kobayashi, H. Tanaka, and H. Kobayashi, *Nature*, **410**, 908 (2001). b) L. Balicas, J. S. Brooks, K. Storr, S. Uji, M. Tokumoto, H. Tanaka, H. Kobayashi, A. Kobayashi, V. Barzykin, and L. P. Gor'kov, *Phys. Rev. Lett.*, **87**, 7002 (2001). c) S. Uji, H. Shinagawa, C. Terakura, T. Terashima, T. Yakabe, Y. Terai. M. Tokumoto, A. Kobayashi, H. Tanaka, and H. Kobayashi, *Phys. Rev. B*, **64**, 24531 (2001). d) L. Balicas, V. Barzykin, K. Storr, J. S. Brooks, M. Tokumoto, S. Uji, H. Tanaka, H. Kobayashi, and A. Kobayashi, *J. Phys. IV France*, **114**, 199 (2004). e) S. Uji, S. Yasuzuka, H. Tanaka, M. Tokumoto, B. Zhang, H. Kobayashi, E. S. Choi, D. Graf, and J. S. Brooks, *J. Phys. IV France*, **114**, 391 (2004). f) J. S. Brooks, S. Uji, E. S. Choi, H. Kobayashi, A. Kobayashi, H. Tanaka, and M. Tokumoto, *J. Phys. IV France*, **114**, 175 (2004).

26 H. Tanaka, T. Adachi, E. Ojima, H. Fujiwara, K. Kato, H. Kobayashi, A. Kobayashi, and P. Cassoux, *J. Am. Chem. Soc.*, **121**, 11243 (1999).

27 a) H. Kobayashi, A. Sato, E. Arai, H. Akutsu, A. Kobayashi, and P. Cassoux, *J. Am. Chem. Soc.*, **119**, 12392 (1997). b) A. Sato, E. Ojima, H. Akutsu, H. Kobayashi, A. Kobayashi, and P. Cassoux, *Chem. Lett.*, **1998**, 673. c) H. Kobayashi, H. Akutsu, E. Ojima, A. Sato, H. Tanaka, A. Kobayashi, and P. Cassoux, *Synth. Met.*, **103**, 1837 (1999).

28 a) L. K. Montgomery, T. Burgin, J. C. Huffman, K. D. Carlson, J. D. Judek, G. A. Yaconi, L. A. Megna, P. R. Mobley, W. K. Kwok, J. M. Williams, J. E. Schirber, D. L. Overmyer, J. Ren, C. Rovira, and M.-H. Whangbo, *Synth. Met.*, **56**, 2090 (1993). b) L. K. Montgomery, B. W. Fravel, J. C. Huffman, C. C. Agosta, and S. A. Ivanov, *Synth. Met.*, **85**, 1521 (1997).

29 V. Gritsenko, H. Tanaka, H. Kobayashi, and A. Kobayashi, *J. Mater. Chem.*, **11**, 2410 (2001).

30 a) E. Ojima, H. Fujiwara, K. Kato, H. Kobayashi, H. Tanaka, A. Kobayashi, M. Tokumoto, and P. Cassoux, *J. Am. Chem. Soc.*, **121**, 5581 (1999). b) H. Fujiwara, E. Fujiwara, Y. Nakazawa, B. Zh. Narymbetov, K. Kato, H. Kobayashi, A. Kobayashi, M. Tokumoto, and P. Cassoux, *J. Am. Chem. Soc.*, **123**, 306 (2001).

31 a) H. Fujiwara, H. Kobayashi, E. Fujiwara, and A. Kobayashi, *J. Am. Chem. Soc.*, **124**, 6816 (2002). b) B. Zhang, H. Tanaka, H. Fujiwara, H. Kobayashi, E. Fujiwara, and A. Kobayashi, *J. Am. Chem. Soc.*, **124**, 9982 (2002).

32 E. Fujiwara, H. Fujiwara, H. Kobayashi, T. Otsuka, and A. Kobayashi, *Adv. Mater.*, **14**, 1376 (2002).

33 T. Otsuka, H.-B. Cui, H. Fujiwara, H. Kobayashi, E. Fujiwara, and A. Kobayashi, *J. Mater. Chem.*, **14**, 1682 (2004).

34 T. Courcet, I. Malfant, K. Pokhodnia, and P. Cassoux, *New J. Chem.*, **1998**, 585.

35 Crystal structure of an isostructural λ'-$(BETS)_2GaBr_4$ salt was reported: H. Tanaka, A. Kobayashi, and H. Kobayashi, *Chem. Lett.*, **1999**, 133.

36 T. Mori, A. Kobayashi, Y. Sasaki, H. Kobayashi, G. Saito, and H. Inokuchi, *Bull. Chem. Soc. Jpn.*, **57**, 627 (1984).

37 a) H. Tajima, A. Kobayashi, T. Naito, and H. Kobayashi, *Solid State Commun.*, **98**, 755 (1996). b) N. Kushch, O. Dyachenko, V. Gritsenko, S. Pesotskii, R. Lyubovskii, P. Cassoux, C. Faulmann, A. Kovalev, M. Kartsovnik, L. Brossard, H. Kobayashi, and A. Kobayashi, *J. Phys. I France*, **6**, 1997 (1996). c) N. Harrison, C. Mielke, D. Rickel, L. Montgomery, C. Gerst, and J. Thompson, *Phys. Rev. B*, **57**, 8751 (1998).

38 C. Hotta and H. Fukuyama, *J. Phys. Soc. Jpn.*, **69**, 2577 (2000).

39 a) L. Balicas, J. S. Brooks, K. Storr, D. Graf, S. Uji, H. Shinagawa, E. Ojima, H. Fujiwara, H. Kobayashi, A. Kobayashi, and M. Tokumoto, *Solid State Commun.*, **116**, 557 (2000). b) S. Uji, H. Shinagawa, Y. Terai, T. Yakabe, C. Terakura, T. Terashima, L. Balicas, J. S. Brooks, E. Ojima, H. Fujiwara, H. Kobayashi, A. Kobayashi, and M. Tokumoto, *Physica B*, **298**, 557 (2001).

40 V. Jaccarino and M. Peter, *Phys. Rev. Lett.*, **9**, 290 (1962).

41 a) T. Konoike, H. Fujiwara, B. Zhang, H. Kobayashi, M. Nishimura, S. Yasuzuka, K. Enomoto, and S. Uji, *J. Phys. IV France*, **114**, 223 (2004). b) T. Konoike, S. Uji, T. Terashima, M. Nishimura, S. Yasuzuka, K. Enomoto, H. Fujiwara, B. Zhang, and H. Kobayashi, *Phys. Rev. B*, **70**, 094514 (2004).

42 O. Cépas, R. H. McKenzie, and J. Merino, *Phys. Rev. B*, **65**, 100502(R) (2002).

43 T. Mori and M. Katsuhara, *J. Phys. Soc. Jpn.*, **71**, 826 (2002).

44 a) M. A. Tanatar, M. Suzuki, T. Ishiguro, H. Fujiwara, and H. Kobayashi, *Physica C*, **388**, 613 (2003). b) M. A. Tanatar, M. Suzuki, T. Ishiguro, H. Tanaka, H. Fujiwara, H. Kobayashi, T. Toito, and J. Yamada, *Synth. Met.*, **137**, 1291 (2003).

45 a) V. A. Bondarenko, M. A. Tanatar, A. E. Kovalev, T. Ishiguro, S. Kagoshima, and S. Uji, *Rev. Sci. Instrum.*, **71**, 3148 (2000). b) M. A. Tanatar, T. Ishiguro, H. Tanaka, and H. Kobayashi, *Phys. Rev. B*, **66**, 134503 (2002).

46 a) T. Otsuka, A. Kobayashi, Y. Miyamoto, J. Kiuchi, N. Wada, E. Ojima, H. Fujiwara, and H. Kobayashi, *Chem. Lett.*, **2000**, 732. b) T. Otsuka, A. Kobayashi, Y. Miyamoto, J. Kiuchi, S. Nakamura, N. Wada, E. Fujiwara, H. Fujiwara, and H. Kobayashi, *J. Solid State Chem.*, **159**, 407 (2001). c) D. Zhang, K. Andres, Ch. Probst, W. Biberacher, N. D. Kushch, and H. Kobayashi, *Solid State Commun.*, **115**, 433 (2000). d) H. Uozaki, T. Sasaki, S. Endo, and N. Toyota, *J. Phys. Soc. Jpn.*, **69**, 2759 (2000).

47 a) H. Kobayashi, H. Akutsu, E. Arai, H. Tanaka, and A. Kobayashi, *Phys. Rev. B*, **56**, R8526 (1997). b) H. Akutsu, K. Kato, E. Ojima, H. Kobayashi, H. Tanaka, A. Kobayashi, and P. Cassoux, *Phys. Rev. B*, **58**, 9294 (1998). c) H. Tanaka, A. Kobayashi, A. Sato, H. Akutsu, and H. Kobayashi, *J. Am. Chem. Soc.*, **121**, 760 (1999).

48 Pratt et al. have determined T_c of κ-$(BETS)_2FeCl_4$ to be 0.17 K by μSR experiments: F. L. Pratt, S. L. Lee, S. J. Blundell, I. M. Marshall, H. Uozaki, and N. Toyota, *Synth. Met.*, **133–134**, 489 (2003).

49 a) B. T. Matthias, E. Corenzwit, J. M. Vandenberg, and H. E. Barz, *Proc. Natl. Acad. Sci. U.S.A.*, **74**, 1334 (1977). b) J. M. Vandenberg and B. T. Matthias, *Proc. Natl. Acad. Sci. U.S.A.*, **74**, 1336 (1977). c) H. Matsumoto and H. Umezawa, *Cryogenics*, **1983**, 37 (1983).

50 a) R. Chevrel, M. Sergent, and J. Prigent, *J. Solid State Chem.*, **3**, 515 (1971). b) Ø. Fischer, *Appl. Phys.*, **16**, 1 (1978). c) M. Ishikawa, Ø. Fischer, and J. Muller, *J. de Phys.*, **C6**, 1379 (1978). d) Ø. Fischer, M. Ishikawa, M. Pelizzone, and A. Treyvaud, *J. de Phys.*, **C5**, 89 (1979).

51 H. C. Ku, F. Acker, and B. T. Matthias, *Phys. Lett.*, **76A**, 399 (1980).

52 a) T. Sugano, T. Fukasaka, and M. Kinoshita, *Synth. Met.*, **41**, 3281 (1991). b) T. Sugimoto, S. Yamaga, M. Nakai, K. Ohmori, M. Tsujii, H. Nakatsuji, and H. Hosoito, *Chem. Lett.*, **1993**, 1361. c) S. Nakatsuji and H. Anzai, *J. Mater. Chem.*, **7**, 2161 (1997). d) R. Kumai, A. Izuoka, and T. Sugawara, *Mol. Cryst. Liq. Cryst.*, **232**, 151 (1993). e) J. Nakazaki, M. M. Matsushita, A. Izuoka, and T. Sugawara, *Tetrahedron Lett.*, **40**, 5027 (1999). f) J. Nakazaki, Y. Ishikawa, A. Izuoka, T. Sugawara, and Y. Kawada, *Chem. Phys. Lett.*, **319**, 385 (2000).

53 a) H. Fujiwara and H. Kobayashi, *Synth. Met.*, **102**, 1740 (1999). b) H. Fujiwara and H. Kobayashi, *Chem. Commun.*, **1999**, 2417. c) H. Fujiwara, E. Ojima, and H. Kobayashi, *Synth. Met.*, **120**, 971 (2001). d) H. Fujiwara, E. Fujiwara, and H. Kobayashi, *Mol. Cryst. Liq. Cryst.*, **380**, 269 (2002). e) H. Fujiwara, E. Fujiwara, and H. Kobayashi, *Synth. Met.*, **133–134**, 359 (2003). f) E. Fujiwara, A. Kobayashi, H. Fujiwara, T. Sugimoto, and H. Kobayashi, *Chem. Lett.*, **33**, 964 (2004).

54 a) H. Fujiwara, E. Fujiwara, and H. Kobayashi, *Chem. Lett.*, **2002**, 1048. b) H. Fujiwara, E. Fujiwara, and H. Kobayashi, *Synth. Met.*, **135–136**, 533 (2003). c) H. Fujiwara, H.-J. Lee, H. Kobayashi, E. Fujiwara, and A. Kobayashi, *Chem. Lett.*, **32**, 482 (2003). d) H.-J. Lee, H.-B. Cui, H. Fujiwara, H. Kobayashi, E. Fujiwara, and A. Kobayashi, *J. Phys. IV France*, **114**, 533 (2004).

55 a) Y. Misaki, T. Matsui, K. Kawakami, H. Nishikawa, T. Yamabe, and M. Shiro, *Chem. Lett.*, **1993**, 1337. b) Y. Misaki, H. Fujiwara, T. Yamabe, T. Mori, H. Mori, and S. Tanaka, *Chem. Lett.*, **1994**, 1653. c) T. Mori, Y. Misaki, H. Fujiwara, and T. Yamabe, *Bull. Chem. Soc. Jpn.*, **67**, 2685 (1994).

56 H. Fujiwara, H.-J. Lee, H.-B. Cui, H. Kobayashi, E. Fujiwara, and A. Kobayashi, *Adv. Mater.*, **16**, 1765 (2004).

Hideki Fujiwara was born in Kishiwada, Osaka in 1969, and received his B.Eng. (1992), M.Eng. (1994), and Dr.Eng. (1999) from Kyoto University. He was appointed as a Research Associate at the Institute for Molecular Science, Okazaki National Research Institutes, in 1996 and moved to the Research Institute for Advanced Science and Technology, Osaka Prefecture University, in 2003. He received the Chemical Society of Japan Award for Young Chemists for 2003. His current research is focused on the development of novel multi-functional materials based on molecular conductors.

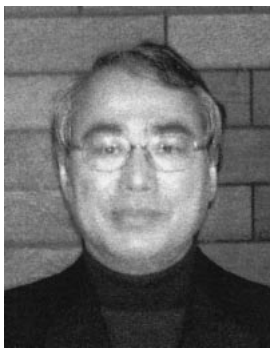

Hayao Kobayashi was born in 1942 in Tokyo, Japan. He studied chemistry at the University of Tokyo. He received his M.S. (1967) and Ph.D. (1970) degrees from the University of Tokyo. He became Lecturer at Toho University in 1971 and promoted to Professor in 1980. He moved in 1995 to Institute for molecular Science in Okazaki. He started his research on molecular conductors when he became a doctor course student in 1967. Since then he studied various molecular conductors, such as TCNQ complexes, partially oxidized 1D platinum complexes, BEDT-TTF, $M(dmit)_2$, DCNQI, and BETS systems and recently single-component molecular metals. His present main interests are in the design and development of multi-functional molecular systems including porous materials with novel electronic functions.